JOURNAL OF MATERIALS SCIENCE **40** (2005) 4199–4219

Extrudate fracture and spheronisation of microcrystalline cellulose pastes

S. L. ROUGH, D. I. WILSON*
Department of Chemical Engineering, University of Cambridge, Pembroke Street, Cambridge, CB2 3RA, UK
E-mail: ian_wilson@cheng.cam.ac.uk

An experimental study of the ram extrusion and subsequent spheronisation of water-based microcrystalline cellulose (MCC) pastes has been performed. The effects of extrusion velocity, die geometry, and paste water content on the integrity of the extrudate produced were investigated. The apparent severity of extrudate fracture increased with decreasing die length/diameter ratio (L/D), and increasing extrusion velocity. The spacing between the fractures was approximately constant for a given set of process conditions, and increased with increasing L/D and decreasing extrusion velocity, whilst the flare of the extrudate fracture segment increased with decreasing L/D and increasing extrusion velocity. Two types of fracture shape were identified, *viz.* knuckle-bones and cups, the occurrence of which is explained in terms of the relative extent of the radial and axial strain release at the surface of the extrudate upon exiting the die.

The shape and size distributions of the corresponding spheronised pellets were analysed and related to the geometry of the extrudate fracture segments. Severe knuckle-bone fracture gave spherical pellets with a wide size distribution. Visibly smooth extrudates gave non-spherical pellets with an apparently narrow size distribution (as measured by sieving). Extrudates displaying the cup type of fracture generated the best quality pellets in terms of both sphericity and size distribution.

1. Introduction

One simple and effective way to deliver a dosage of drug in a controlled manner is to use small pellets, ideally spheres of 1–2 mm in diameter, that are compacted or filled into tablets and capsules. The majority of each pellet comprises an excipient, such as lactose or microcrystalline cellulose (MCC), containing or coated with a small amount of active ingredient. Sphericity and a narrow size distribution of the constituent pellets are important for coating quality, dose uniformity and reproducibility, as well as allowing for good flow properties and uniform packing of the particulate material [1]. One of the main methods of forming such pellets is that of extrusion-spheronisation [2], where paste extrudates are introduced onto a rotating friction plate, the action of which breaks up the extrudates and shapes the segments into spheroids of roughly the same diameter of the extrusion screen or die orifice [3, 4].

Conine and Hadley [5] suggested a basic criterion for successful spheronisation, in that the extrudate must be able to break up into sections that are plastic enough to be rounded by the forces imposed by the rotating friction plate. The stages in spheronisation were outlined by Rowe [6] using descriptions of the shape of the pellets, progressing from a cylinder, round-ended cylinder, dumb-bell, ellipse and finally to a sphere. Chapman *et al*. [7] added that the shaping process is a result of densification as the segment of extrudate is compressed along its length; however, neither Kleinebudde *et al*. [8] nor Galland *et al*. [9] observed any densification during the spheronisation of MCC paste extrudates, presumably because the extrudates had already attained a minimum porosity. Baert and Remon [10] suggested a different spheronisation mechanism, in which the round-ended cylinders are twisted and broken into two parts, each with a round and a flat side. The edges of the flat side subsequently fold together to form a sphere with a dimple.

It is imperative that the extrudate to be spheronised is of a suitable moisture content—too wet a mixture will result in uncontrollable agglomeration, whereas for dry mixes, the pellets will fail to round and thus remain as cylinders [11]. A low moisture content can also generate a large amount of small attrition product, or 'fines' [12, 13]. Thus it is important that the extrudate maintains an homogeneous water content, since any variation will result in pellets with a wide size distribution and non-uniform shape [14].

Whilst screen extruders are employed industrially for the continuous production of extrudates, research

* Author to whom all correspondence should be addressed.

workers make use of the ram extruder, which is essentially a batch process that allows for the controlled study of extrusion under a variety of processing and design conditions. One of the first major research studies on ram extrusion-spheronisation of pharmaceutical pastes was that by Harrison [15], where the effects of the die geometry and process conditions on the surface integrity of MCC/lactose paste extrudates were investigated and related to the attributes of the subsequent spheronised product. He observed that high extrusion velocities produced extrudates with a rough surface, and for a die length/diameter ratio (*L/D*) less than or equal to one, the extrudate became what is commonly termed 'shark-skinned', a surface impairment characterised by regular circumferential cracks. Both types of defect produced brittle and short extrudates, and the defects became more pronounced with increasing extrusion velocity. This produced poor quality pellets since the extrudate broke up unevenly in the spheroniser resulting in many fines and a wide size distribution. He suggested that the surface impairments were a result of an imbalance of stresses on the extrudate surface as it exited the die. For the screen extrusion of MCC-based pastes, it has also been observed that a decrease in the screen thickness often led to highly porous, surface-impaired extrudates (e.g. [16, 17, 18, 19, 20]). This was attributed to a higher densification of the paste occurring in a screen of greater thickness.

An extensive experimental study of the fracture of pastes during ram extrusion fracture was performed by Domanti [21], some results of which were reported in Domanti and Bridgwater [22]. They observed that the depth of fracture of alumina/glucose paste extrudates increased with decreasing *L/D*, increasing extrusion velocity, decreasing extrusion ratio (barrel diameter/die diameter), and by reducing the taper of the die entry. They also showed that the fracture spacing along the extrudate was constant and approximately equal to $D/2$, regardless of the extrusion velocity and die length. This periodicity was also reported by Amarasinghe and Wilson [23] and Russell *et al.* [24] for a variety of pastes, and can also be observed in some of the photographs of Harrison [15]. Periodic extrusion defects are not only observed in paste processing, but have also been reported for metals (e.g. [25]) and polymer melts (e.g. [26, 27, 28, 29]). Much work has been performed on polymers in an attempt to understand the related mechanisms of melt extrusion fracture.

Since the integrity of the paste extrudate has been shown to affect the shape and size distribution of the spheronised pellets (e.g. [12, 30, 31]), fracture or surface impairment of extrudates prior to spheronisation has always been anathema within pharmaceutical research. For example, Harrison *et al.* [32] state that extrudate surface impairments such as roughness and sharkskinning "will severely mar the qualities of the product and should be avoided wherever possible". Mesiha and Vallés [33] also conclude that "the absence of surface defects promotes uniform breakage of the extrudate during spheronisation and minimises fine particles resulting from the segmentation of deep ridges". These studies thus suggest that smooth, defect-free extrudates are necessary for successful spheronisation. However, Pinto *et al.* [12] add that "not all good extrudates will produce a good sphere". Similarly, one may ask the following: do all extrudates with poor surface quality produce poor quality spheres ? It is this question that the present work attempts to address by investigating the relationship between the quality of water-based MCC paste extrudates and the spheronised product, and by determining the influence of the processing conditions and material properties upon the extrudate surface impairments. From these results, a mechanism for extrudate fracture is also discussed in terms of previous paste and polymer melt extrusion studies.

2. Materials and methods

2.1. Paste preparation

The pastes studied consisted of deionised water and a standard excipient MCC powder (Avicel PH-101, Sigma-Aldrich, Germany). Two paste compositions that led to successful extrusion-spheronisation (55 and 50 wt% water-MCC on a wet basis, corresponding to solids volume fractions of 0.35 and 0.40 respectively for saturated pastes) were prepared using an A200 Hobart planetary mixer. The dry powder (ranging between 300–500 g) was loaded into the mixer bowl and the water slowly poured onto the stirred powder bed. The paste was mixed for 10 min, during which time any caked mixture was disrupted from the sides and bottom of the bowl using a plastic spatula at 2, 5 and 8 min mixing time. The paste was then pugged through a 4 mm diameter holed die plate in order to break up agglomerates, and was stored in a sealed plastic bag at room temperature for 2 h before extrusion.

2.2. Extrusion and spheronisation

A computer-controlled ram extruder (Dartec A100 screw strain frame, Stourbridge, UK), incorporating a cylindrical 25 mm internal diameter stainless steel barrel and various concentric cylindrical square-entry dies, was used to produce the paste extrudates. A detailed description of the apparatus is reported elsewhere [34]. About 70–75 g of paste was loaded into the barrel using a scoop and funnel, and was tamped down by hand every $\sim$ 25 g to produce a billet about 150 mm in height. A ram attached to the cross-head of the strain frame was used to pre-compact the paste to a mean stress of 1 MPa. The ram velocity was set at a given value, and the paste was extruded through the die for a ram displacement of 100 mm. A relatively high ram velocity was used (ranging from 0.89 to 10 mm s^{-1}) in order to minimise any re-distribution of water within the barrel paste during the compaction stage, thus producing extrudates of homogeneous water content throughout the extrusion [35]. Profiles of extrusion force against ram displacement were relatively steady, indicating that liquid phase redistribution was minimal. Details of the

TABLE I Values of the average extrusion pressure and their variation obtained for 55 wt% and 50 wt% water-MCC paste at various mean extrusion velocities (V) and die geometries

		55 wt%						55 wt%	
		$D = 3$ mm		$D = 2$ mm		$D = 1$ mm		$D = 3$ mm	
V (m s^{-1})	L/D	Extrusion pressure (MPa)	Wall shear stress (MPa)	Extrusion pressure (MPa)	Wall shear stress (MPa)	Extrusion pressure (MPa)	Wall shear stress (MPa)	Extrusion pressure (MPa)	Wall shear stress (MPa)
140	1	4.6 ± 0.24*	0.21	5.4 ± 0.71	0.28	–	–	7.4 ± 0.58	0.35
	2	5.1 ± 0.47		6.5 ± 1.4		–		9.4 ± 0.31*	
	4	6.9 ± 0.04		8.4 ± 1.4		–		13 ± 1.4	
	8	10 ± 0.20*		13 ± 0.98		–		17 ± 1.5	
	16	17 ± 0.02		22 ± 1.0*		–		24 ± 0.72	
350	1	4.5 ± 0.24*	0.29	–	–	–	–	8.9 ± 0.36	0.44
	2	5.3 ± 0.29*		–		–		10 ± 0.29*	
	4	7.3 ± 0.14*		–		–		15 ± 0.74	
	8	11 ± 0.00		–		–		21 ± 1.6	
	16	22 ± 0.63*		–		–		35 ± 1.7	
690	1	4.6 ± 0.37*	0.33	5.3 ± 0.04	0.37	–	0.32	9.0 ± 0.24	0.48
	2	5.7 ± 0.0		7.1 ± 0.55		8.9 ± 0.77		10 ± 0.60*	
	4	8.0 ± 0.65*		9.4 ± 0.67		11 ± 0.51		15 ± 0.92	
	8	12 ± 0.43		15 ± 0.14*		17 ± 0.91		22 ± 1.6	
	16	24 ± 0.10*		28 ± 0.15		–		38 ± 1.1*	

*Indicates a negative pressure-displacement gradient, i.e. the extrusion pressure decreases with increasing ram displacement. The die wall shear stress values are obtained from Bagley plots.

extrusion pressures are given in Table I for various die geometries and mean die land paste velocities, V; values of the die wall shear stresses are also listed, as estimated from 'Bagley' plots of extrusion pressure vs. L/D. The apparent shear rates were calculated as ranging between 370 and 1850 s^{-1} for the 3 mm dies, 556 and 2780 s^{-1} for the 2 mm dies, and 5560 s^{-1} for the 1 mm dies. These values are reported here for comparison with other studies but are not intended to characterise the flow reliably as some wall slip is expected in these systems [15].

The extrudate (∼30–50 g) was collected, and ∼0.5 g was reserved for microscope analysis. The remaining extrudate was spheronised using a bench-top 120 Spheroniser (Caleva Process Solutions Ltd., Dorset, UK) incorporating a 120 mm diameter cross-hatched friction plate (3 mm pitched truncated square pyramids, 1 mm high). The extrudates were spheronised for 2 min at a constant plate rotational speed of 1600 rpm. The resulting pellets were carefully removed from the spheroniser drum using a soft-haired brush, and dried at atmospheric pressure in an oven at 60°C for 20 h in order to allow for further characterisation without significant deformation.

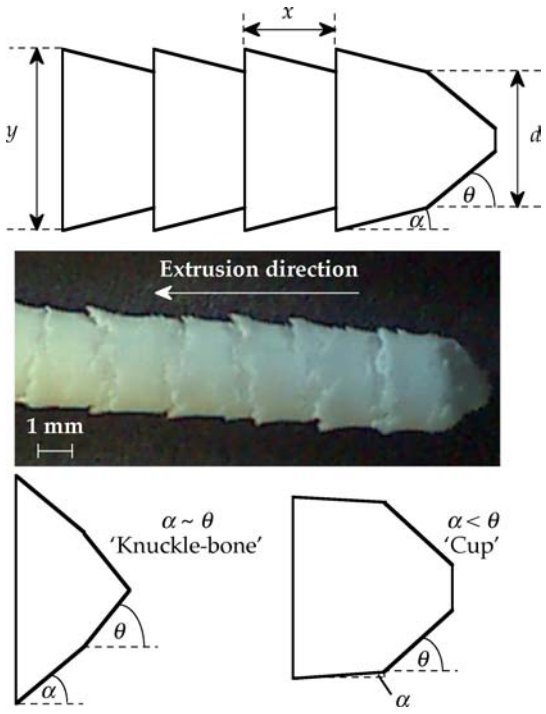

Figure 1 An example of a fractured paste extrudate (50 wt% water-MCC extruded at $V = 350$ mm s^{-1} through a 3 mm diameter die with $L/D = 4$), and a schematic representation of the fracture geometry introducing the symbols used in the text.

2.3. Extrudate and pellet characterisation

The extrudates and dried pellets were viewed optically using an Intel® Play™ QX3™ computer microscope (Mattel, California, USA). The extrudates were analysed as soon as possible in order to minimise shrinkage due to drying. Geometrical features of the extrudates, as defined in Fig. 1, were determined by examining enlarged microscope pictures of ∼20 mm of extrudate (including a ± 0.25 mm scale) and averaging over a number of measurements. The values ascertained in this manner included the fracture spacing, x, and the extrudate flare, y.

The pellet size distribution of each test sample was determined using a $2^{1/2}$ progression of sieves, with an additional $2^{1/4}$ progression around the modal diameter. The sieving was carried out by hand, and the mass of each fraction collected was determined to within ±0.01 g. The shrinkage of the pellets due to drying was measured for a number of different

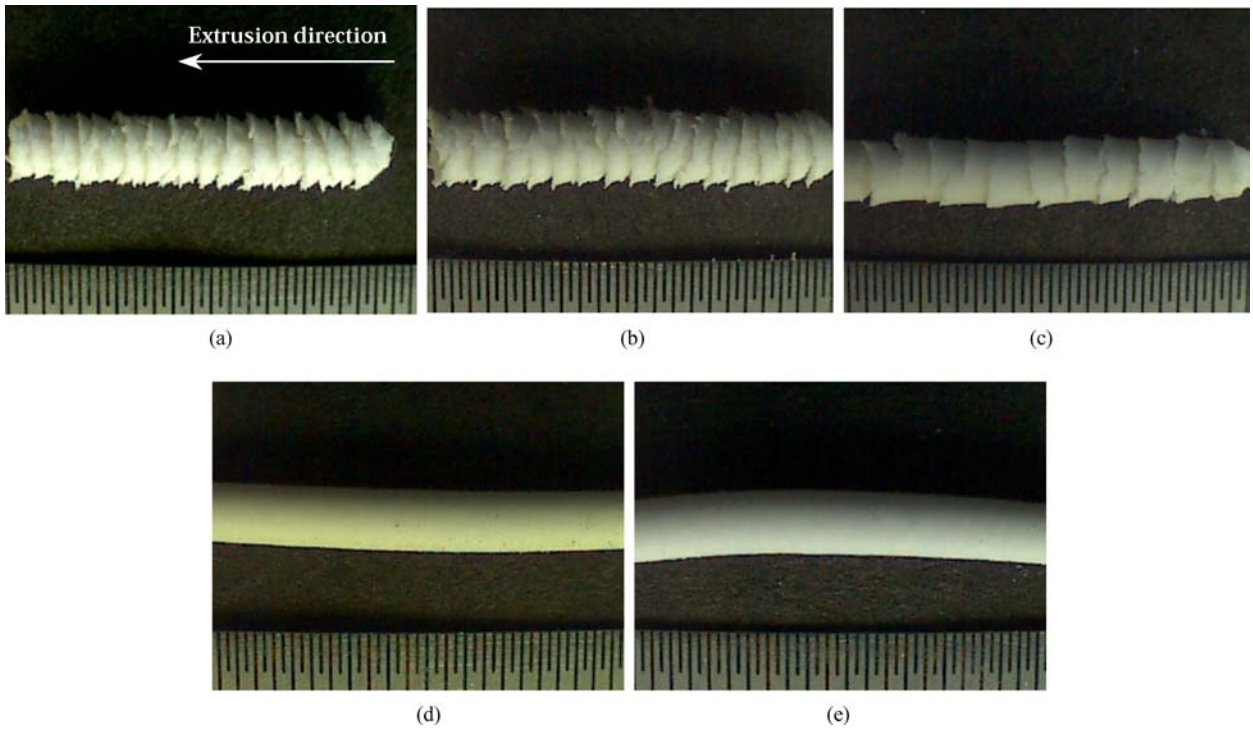

Figure 2 Extrudates of 55 wt% water-MCC extruded at $V = 140$ mm s^{-1} through a 3 mm diameter die with $L/D =$ [a] 1, [b] 2, [c] 4, [d] 8 and [e] 16 mm. The scale shows 0.5 mm divisions.

sized pellets using vernier callipers, and was on average ∼22 and 27% for the 55 and 50 wt% water-MCC compositions respectively. It was assumed that the shrinkage was independent of pellet size and shape, and occurred homogeneously throughout a given pellet.

3. Results

3.1. Effect of die length

Fig. 2 shows the extrudates of a 55 wt% water-MCC paste extruded through a 3 mm diameter die with *L/D* equal to 1, 2, 4, 8 and 16 at V = 140 mm s^{-1} (corresponding to a ram velocity of 2 mm s^{-1}). Regularly spaced fractures occur for $L/D = 1$, 2 and 4, whereas an apparently smooth extrudate is formed for $L/D = 8$ and 16, with some very faint surface fractures visible occasionally. Repeat experiments confirmed the reproducibility of the observed fracture geometries. For the two shortest dies, the extrudate broke under gravity whist leaving the die into segments ∼15 mm (∼5 diameters) in length, whereas the smooth extrudates broke downstream of the die exit upon hitting the base of the collection beaker. The surface outline of the fractures appear quite ragged for the shortest die, becoming smoother with increasing die length. Values of the measured geometrical features of the extrudates are listed in Table II. The fracture spacing (x) increases with increasing die length, with the $L/D = 2$ die producing a spacing of $D/2$. As the die length increases, the extrudate flare (y) decreases from 4 mm to the value of the die diameter (3 mm) for the smooth extrudates. A corresponding decreasing trend in the extrudate 'skirt' angle α (see Fig. 1) is also apparent from the micrographs, although a numerical value for this feature could not be assigned with certainty. However, by assuming that d is equal to the die diameter (i.e. 3 mm), then α can be represented by $\tan^{-1}\{(y - 3)/2x\}$. This term (now symbolised by α') is listed in Table II, and shows a decreasing trend with increasing die length; thus α' may be considered as a measure of what is commonly called the 'severity' of fracture. Upon drying, the extrudate samples that fractured could be easily broken by hand into their constitutive fracture sections, with the two shorter die lengths producing 'knuckle-bone' shaped portions (i.e. $\alpha \sim \theta$, see Fig. 1) whereas the $L/D = 4$ extrudate produced portions more in the shape of a 'cup' (i.e. $\alpha < \theta$).

Micrographs of the corresponding spheronised extrudates are illustrated in Fig. 3. For $L/D = 1$ and 2 (knuckle-bone fractures), the pellets are fairly well-formed and spherical with few satellites and surface depressions. For $L/D = 4$ (cup fractures), the spheres formed are noticeably larger, whereas a number of ellipses and dumb-bells (some up to ∼6 mm in length) are evident for the two longest dies which formed the smooth extrudate. The size distributions of the pellet samples are shown in Fig. 4. The sample produced by the shortest die ($L/D = 1$) has a broad size distribution, with approximately equal mass fractions for pellet diameters ranging between 1.00 and 2.36 mm. For $L/D = 2$, the distribution is once again wide, although a modal diameter within the 2.36–2.80 mm size fraction is now apparent. (Assuming 22% linear shrinkage on drying, this corresponds to a wet size fraction of 3.0–3.6 mm). The same size fraction contains the modal diameter for the $L/D = 4$ sample, although the distribution is

TABLE II Extrudate geometry (as defined in Fig. 1) of 55 wt% and 50 wt% water-MCC pastes extruded through a 3 mm die at various mean extrusion velocities (V) and die length/diameter ratios (L/D).

		55 wt%				50 wt%			
V (mm s^{-1})	L/D	Shape	x (mm)	y (mm)	$\alpha' = \tan^{-1}\left(\frac{y-3}{2x}\right)/(^\circ)$	Shape	x (mm)	y (mm)	$\alpha' = \tan^{-1}\left(\frac{y-3}{2x}\right)/(^\circ)$
140	1	K	1.25	4.0	22	K	1.25	4.75	35
	2	K	1.5	4.0	18	K/C	1.5	4.5	27
	4	C	2.0	3.5	7	C/S	2.25	3.0	0
	8	S	•	3.0	0	S	•	2.75	0
	16	S	•	3.0	0	S	•	2.75	0
	1	K	1.0	4.0	27	K	1.25	4.75	35
350	2	K	1.25	4.0	22	K/C	1.5	4.5	27
	4	K/C	1.25	4.0	22	C	1.75	3.25	4
	8	C	1.5	4.0	18	C	1.75	3.0	0
	16	C	1.5	3.5	9	C	1.75	3.0	0
690	1	K	1.0	4.25	32	K	1.25	4.75	35
	2	K	1.25	4.25	27	K/C	1.5	4.5	27
	4	K	1.25	4.25	27	K/C	1.5	3.5	9
	8	K/C	1.25	4.25	27	C	1.5	3.5	9
	16	C	1.5	3.75	7	C	1.5	3.25	5

Fracture shapes represented by K = Knuckle-bone, C = Cup, S = Smooth.

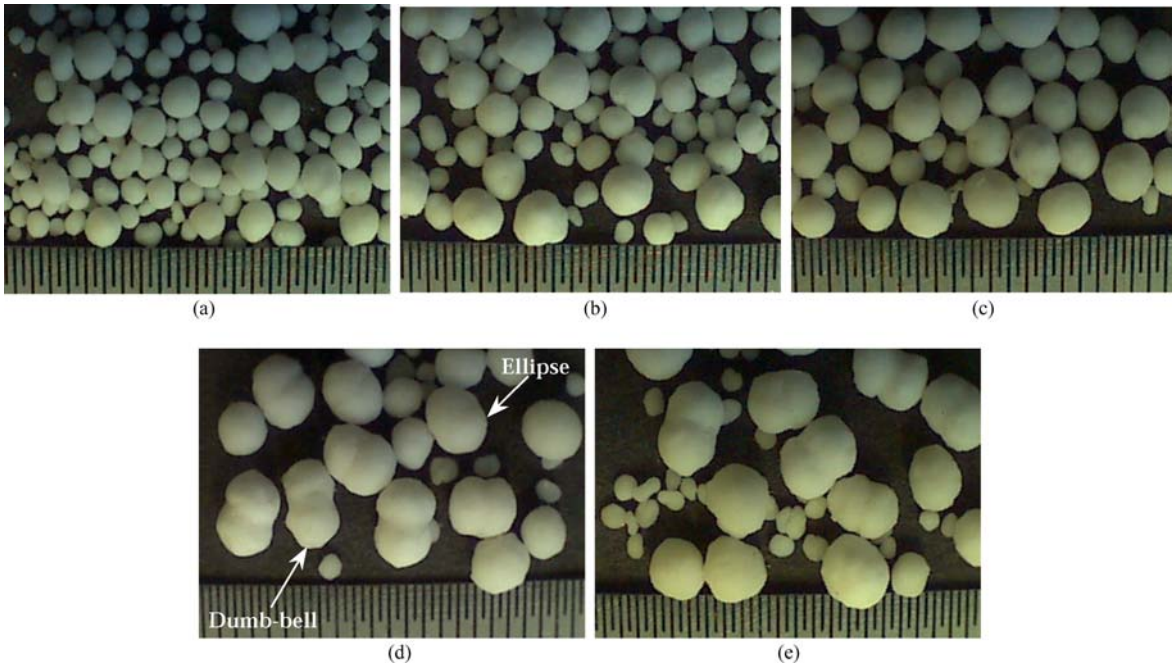

Figure 3 Dried pellets obtained from the spheronisation of 55 wt% water-MCC extruded at $V = 140$ mm s^{-1} through a 3 mm diameter die with L/D = [a] 1, [b] 2, [c] 4, [d] 8 and [e] 16 mm.

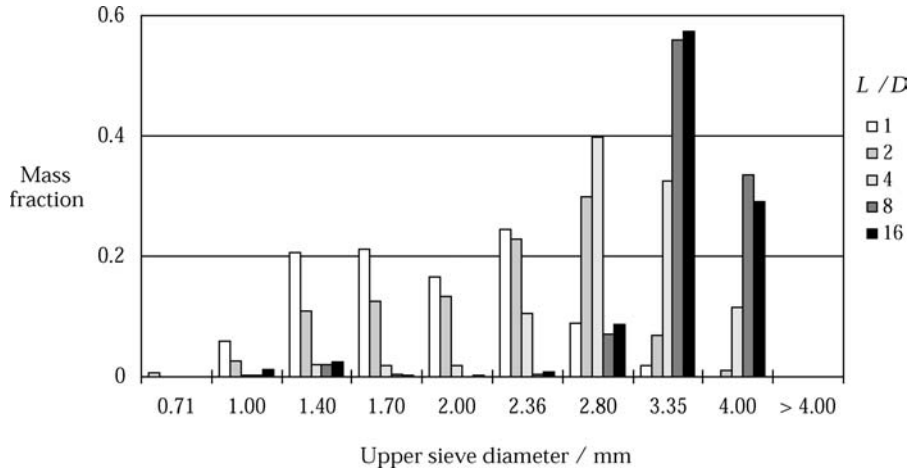

Figure 4 Size distributions in terms of mass fraction of dried pellets obtained from the spheronisation of 55 wt% water-MCC extruded at $V = 140$ mm s^{-1} through a 3 mm diameter die with L/D = 1, 2, 4, 8 and 16.

now skewed to the right. As the die lengths are further increased, the pellet size distributions shift further to the right, become narrower, and have a modal diameter within the 2.80–3.35 mm size fraction (3.6–4.3 mm wet), although a number of fines are still present. The two longest dies appear to produce similar pellet size distributions in terms of the sieve diameter. Extended spheronisation of the $L/D = 16$ smooth extrudate (up to 10 min, results not presented here) showed that the ellipses and dumb-bells did eventually attain a spherical form (confirmed by a Camsizer® digital image processing system, Retsch Technology, Germany), although the size distributions of the later samples were distinctly bimodal, e.g. the 10 min sample gave peaks at sieve diameters of 1.8 and 2.7 mm, the lower diameter modal peak being due to coalescence of fines.

A rough estimation of the mean size of the pellets formed from the fractured extrudates can be obtained using the measurements of the fracture shape geometry. Assuming that there is no densification of the paste during spheronisation, and estimating the shape of the fracture segment as a cylinder of diameter $(y + D)/2$ and length x, then the diameter of a sphere, δ, produced from such a cylinder is given by

$$\delta = \sqrt[3]{\frac{3x(y + D)^2}{8}} \quad (1)$$

For the fractures obtained with the $D = 3$ mm dies at the lowest extrusion velocity, using the data in Table II, δ is calculated as 2.8, 3.0 and 3.2 mm for $L/D = 1, 2$ and 4 respectively. These calculations show that the fracture segments are able to form spheres with diameters approximately equal to that of the die, whereas the apparently smooth extrudates generate consistently larger pellets (Fig. 4), indicating that fracture extrusion-spheronisation allows some control over the pellet size distribution.

3.2. Effect of extrusion velocity

The effect of increasing the extrusion velocity was investigated for the same paste and die geometry as described in Section 3.1. The chosen additional extrusion velocities (V) were 350 and 690 mm s^{-1} (corresponding to ram velocities of 5 and 10 mm s^{-1} respectively). For these two velocities, regularly spaced fractures occurred for all L/D values tested. Examples of the extrudates produced at all three velocities are displayed in Figs 5 and 6, and show that the apparent severity of the fractures increases with increasing extrusion velocity for L/D ratios of 4, 8 and 16. Fractures produced with the two shortest dies were of similar appearance to those shown in Fig. 2a and b. The measured geometrical features are once again listed in Table II. For a given velocity, the increase in x and decrease in y and α' with increasing die length is still present. For any given L/D, the two higher velocities yield a smaller value for x when compared with the previous 140 mm s^{-1} velocity data. y and α' also appear to have an increasing trend with increasing extrusion velocity, which corresponds to the visual interpretation of increasing fracture severity. Table II also shows that

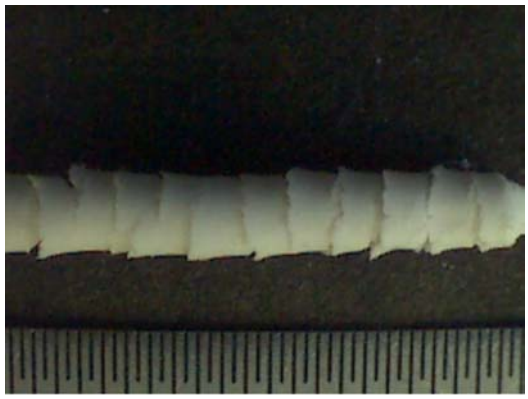

(a)

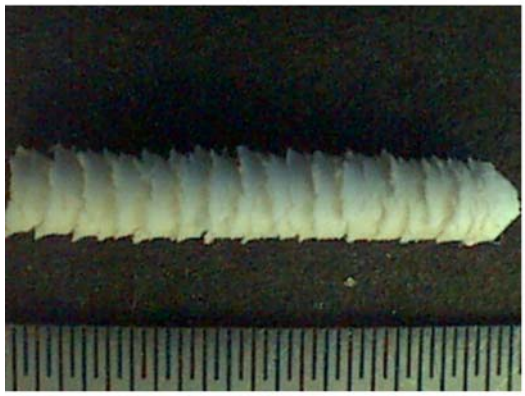

(b)

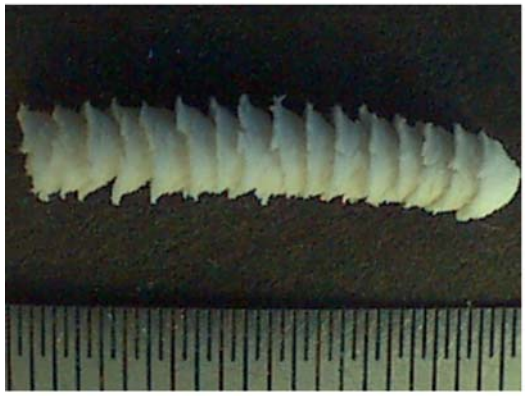

(c)

Figure 5 Extrudates of 55 wt% water-MCC extruded through a 3 mm diameter die with $L/D = 4$ at V = [a] 140, [b] 350 and [c] 690 mm s^{-1}.

knuckle-bones are more likely to be produced as the extrusion velocity increases. Using Eq. (1), the corresponding spheronised pellet diameters are predicted as 2.6 and 2.7 mm for the shortest die, and 2.9 mm for the longest die, at the two higher velocities. Occasional 'fir-tree' fractures (Fig. 7) were also produced at the higher velocities, more so for the shorter dies, although they constituted <5 wt% of the total extrudate sample collected.

For $L/D = 1$ and 2, the pellets formed at the two higher velocities were found to have similar morphologies to those formed at the lower velocity, as shown in Fig. 3a and b, whereas for $L/D = 4$, the pellets were more irregularly shaped. For the two shortest dies, the corresponding size distributions for each velocity are similar, as illustrated in Fig. 8a and b. For $L/D = 4$ and 8, the size distribution is broader for the two

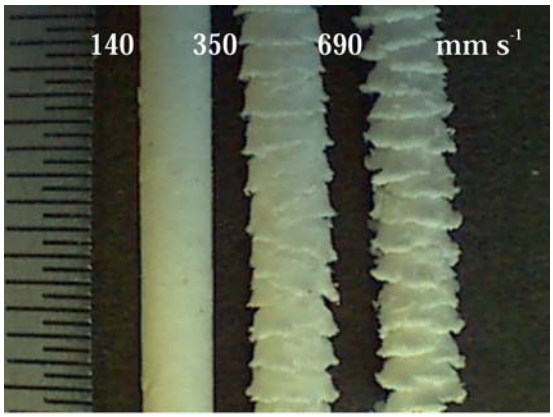

(a)

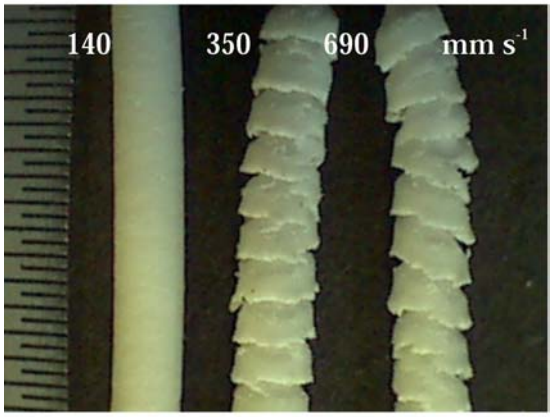

(b)

Figure 6 Extrudates of 55 wt% water-MCC extruded at $V = 140$, 350 and 690 mm s^{-1} through a 3 mm diameter die with $L/D =$ [a] 8 and [b] 16.

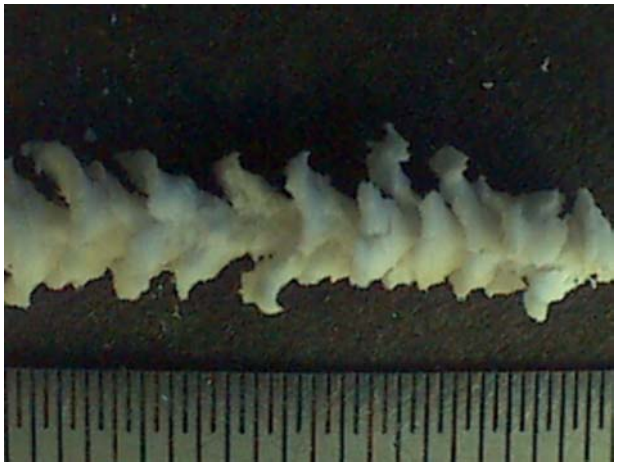

Figure 7 An example of a 'fir-tree' type of fracture, obtained from the extrusion of 55 wt% water-MCC at $V = 690$ mm s^{-1} through a 3 mm diameter die with $L/D = 4$.

highest velocities (see Fig. 8c and d), and is similar to the distributions for $L/D = 1$ and 2, perhaps even bimodal. For the two longest dies, the pellet morphology was markedly different at the higher extrusion velocities. For $L/D = 8$, only one or two dumb-bells were formed at the higher velocities, the rest of the pellets being well-formed spheres and ellipses, although some were dimpled. The number of dimpled pellets increased for the $L/D = 16$ sample, although no dumb-bells were formed at the highest velocity, as displayed in Fig. 9 (*cf.* Fig. 3e). The change in pellet morphology corresponds to the appearance of knuckle-bone and cup fractures as opposed to the visibly smooth extrudates formed at the lowest velocity. The pellet size distribution in Fig. 8e also shows a decrease in value for the modal diameter at the two higher velocities, as well as a decrease in the amount of fines produced. These data, along with the results from Section 3.1, indicate that cup shaped segments are the best type of fracture in terms of generating spherical pellets of narrow size distribution.

3.3. Effect of paste water content

The results from the extrusion/spheronisation of a 50 wt% water-MCC paste were compared with those for the 55 wt% paste. The drier paste required larger extrusion pressures, and the data yielded larger wall shear stress terms for a given velocity and die geometry (Table I). For the lowest velocity, the extrudates produced with $L/D = 1$, 2 and 4 are displayed in Fig. 10. The fracture shapes are similar to that for the 55 wt% paste (*cf.* Fig. 2a–c), although the apparent severity of fracture for the $L/D = 4$ sample is significantly less. Smooth extrudates were produced for $L/D = 8$ and 16 at the lowest velocity, although very faint surface fractures were evident occasionally. Micrographs of the corresponding pellets are shown in Fig. 11. For the two shortest dies, many of the spherical pellets formed were dimpled. For $L/D = 4$, some of the spheres were dimpled and a few dumb-bells were present (<5% by volume). For the two longest dies, the pellets consisted mainly of rough-edged dumb-bells and cylinders up to ~5 mm in size (>90% by volume), with a few spheres present, some dimpled. Comparing these morphologies with the pellets obtained from the 55 wt% paste (Fig. 3), the drier paste produces poorly shaped pellets, with dimples for the shorter dies and more dumb-bells and cylinders for the longer dies. The size distributions for the two pastes are compared in Fig. 12. For all die lengths, the drier paste produces more fines when spheronised, accompanied by a shift in size distribution to the left, although it should be noted that the 50 wt% paste shrinks by 27% during drying as opposed to 22% for the 55 wt% paste. The two shortest dies appear to produce a modal diameter value within the size fraction 1.00–1.40 mm (1.4–1.9 mm wet). For $L/D = 4$, 8 and 16, the distribution is also narrower around the modal value, and the two longest dies show a decrease in the value of the modal diameter compared to that of the 55 wt% sample, although the peaks may coincide since the 50 wt% paste shrinks more during drying.

Examples of the 50 wt% extrudates produced at all three extrusion velocities for the longer dies ($L/D =$ 4, 8 and 16) are displayed in Fig. 13, and show that the apparent severity of the fractures increases with increasing extrusion velocity for a given L/D ratio. The severity does, however, appear less than that for the 55 wt% paste as displayed in Figs 5 and 6. These visual interpretations are borne out by the comparison of the values of x, y and α' in Table II for $L/D = 4$, 8 and 16, and also the fracture shape (i.e. knuckle-bone vs. cup). For the two shortest dies, the velocity had no measurable

effect upon the fracture geometry, although the values of x, y and α' were equal to or larger than those for the corresponding 55 wt% samples. For $L/D = 1, 2$ and 4, the 50 wt% pellets formed at the two higher velocities were found to have similar morphologies to those formed at the lower velocity, as shown in Fig. 11a–c. For $L/D = 8$ and 16, a smaller number of dumb-bells and cylinders were produced at the highest velocity (<1% by volume), and the pellets consisted mainly of dimpled spheres. For the 50 wt% paste at any given L/D ratio, it was found that an increase in extrusion velocity had no major effect upon the pellet sizes as shown in Fig. 12, although the two highest velocities produced slightly wider distributions. Fig. 14 compares the size distributions for the two pastes extruded at the highest velocity with $L/D = 4, 8$ and 16, and shows that the 50 wt% paste begins to attain a narrower distribution about the modal diameter at $L/D = 4$, whereas the 55 wt% paste does so at $L/D = 16$. This again coincides with the onset of cup fractures.

3.4. Effect of die diameter

Extrusions were conducted with the 55 wt% water-MCC paste using dies of diameter 2 mm and 1 mm, with $L/D = 1, 2, 4, 8$ and 16 for the former, and $L/D = 2, 4$ and 8 for the latter. The ram velocities were altered accordingly in an attempt to maintain the die land extrusion velocities, V, used in the 3 mm diameter experimental series. The new ram velocities were

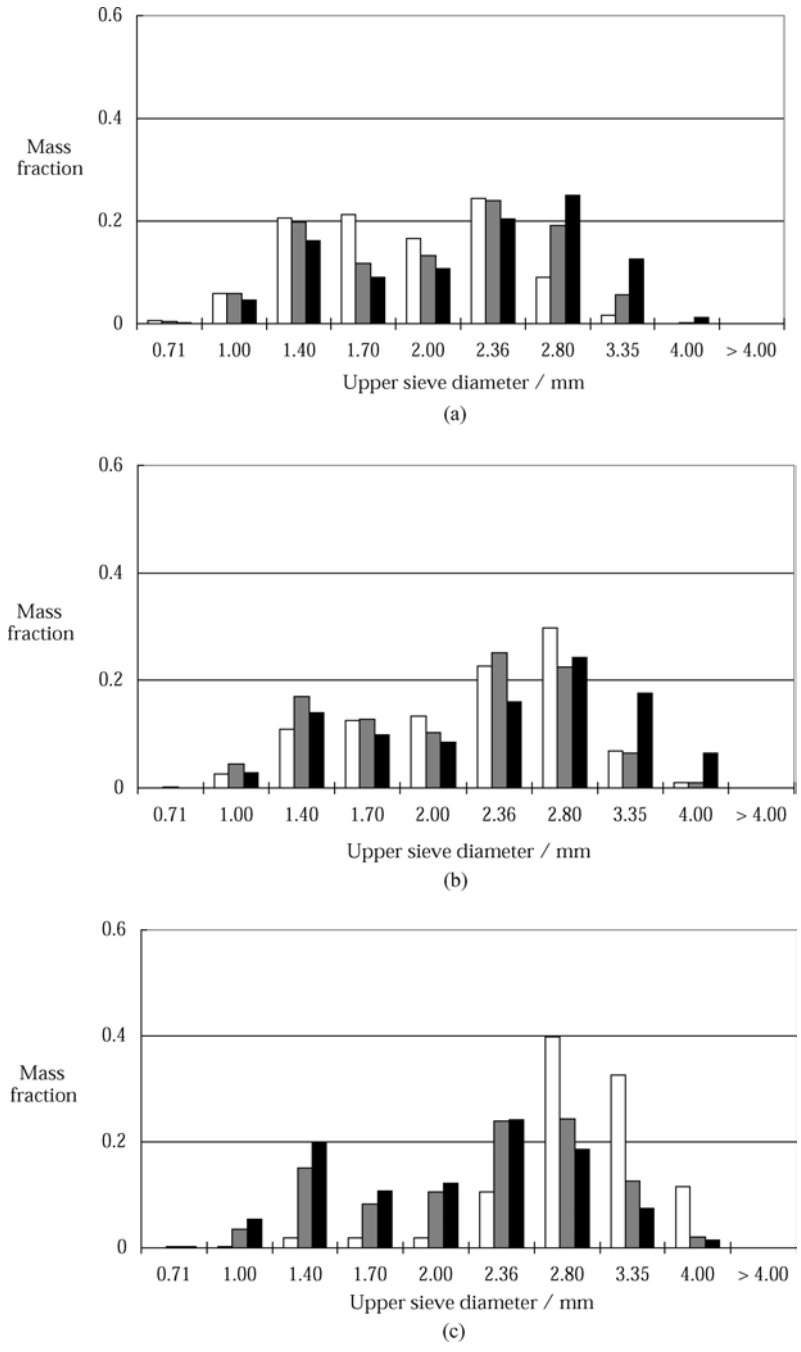

Figure 8 Size distributions in terms of mass fraction of dried pellets obtained from the spheronisation of 55 wt% water-MCC extruded through a 3 mm diameter die at $V = 140$ (□), 350 (▩), and 690 (■) mm s^{-1} with L/D = [a] 1, [b] 2, [c] 4, [d] 8 and [e] 16. (*Continued*.)

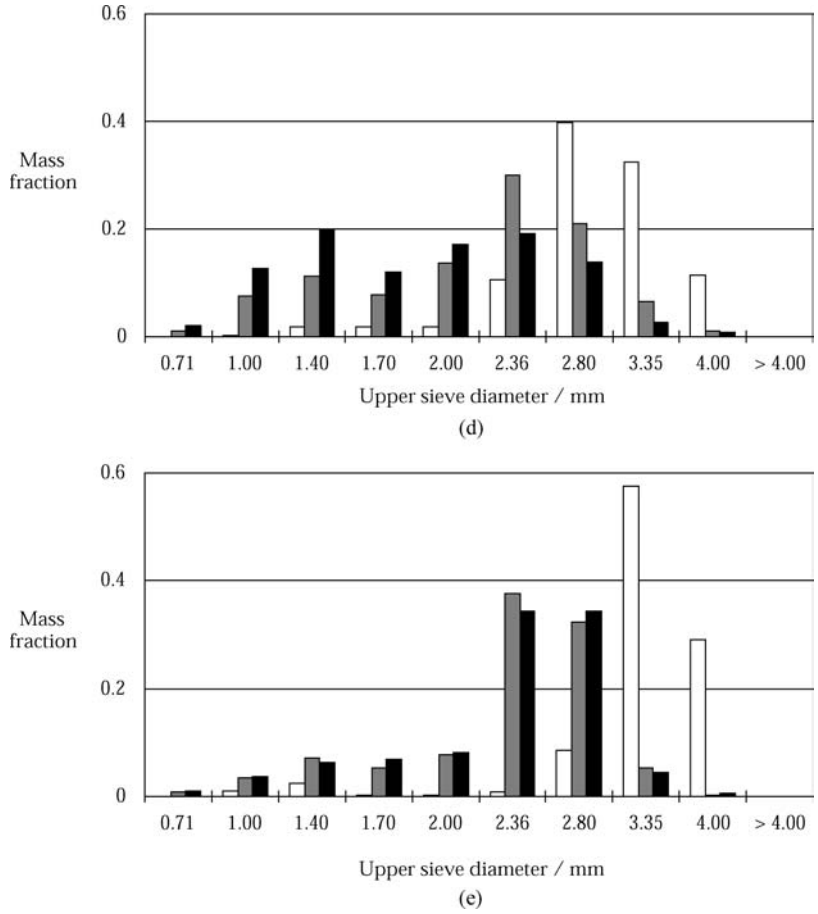

Figure 8 (*Continued*).

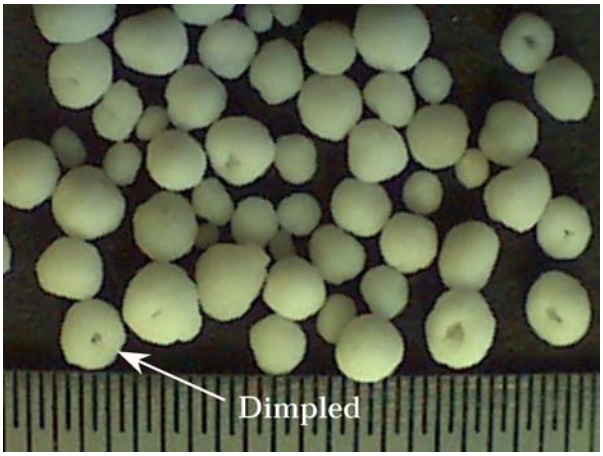

Figure 9 Dried pellets obtained from the spheronisation of 55 wt% water-MCC extruded at $V = 690$ mm s^{-1} through a 3 mm diameter die with $L/D = 16$.

calculated assuming continuity in paste volumetric flowrate, and hence ignored any density changes that may occur during extrusion. With this in mind, for a given L/D ratio, then the die wall shear rate may not be equal when comparing extrusions using different die diameters, and so any comparison of fracture geometry must be treated with caution. However, the extent of fracture of the individual extrudates may still be related to the morphology and size distribution of the spheronised product. Only the highest extrusion velocity was used for the 1 mm diameter die (corresponding to a ram velocity of 1.11 mm s^{-1}) in order to avoid the effects of water migration that were apparent with this die at the two lowest velocities.

For the 2 mm diameter dies, the extrudates fractured forming knuckle-bone shapes for all velocities and L/D values studied, and all the extrudates had flares of $y = 3.0$ mm and fracture spacings of $x = 1.0$ mm ($\delta = 2.1$ mm from Equation 1). No cup fractures or smooth extrudates were formed, as observed for the corresponding 3 mm die experiments, which implies that the extent of fracture is not simply a function of the die wall shear rate. Table I shows that the values obtained for the wall shear stress in the 2 mm diameter dies were larger than those in the 3 mm dies for a given extrusion velocity. An example of the extrudates produced at the lowest and highest velocities is displayed in Fig. 15 for $L/D = 8$, and the fractures are visibly more severe at the highest velocity, although this could not be monitored quantitatively to within measurement error. For $L/D = 1, 2$ and 4, the morphology of the pellets was similar at each velocity, being that of near-spherical pellets, some with dimples (e.g. see Fig. 16a and b). For $L/D = 8$ and 16, the lowest velocity produced many ellipses and some dumb-bells, whereas the highest velocity yielded mostly spheres, many with dimples (e.g. see Fig. 16c and d). The corresponding pellet size distributions are illustrated in Fig. 17, and for the lowest velocity, the distributions for $L/D = 1, 2$ and 4 are similar, with the modal diameter occurring within the size fraction 1.40–1.70 mm (1.8–2.2 mm wet). For

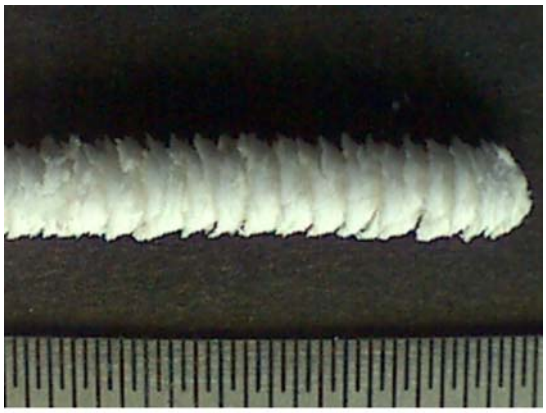

(a)

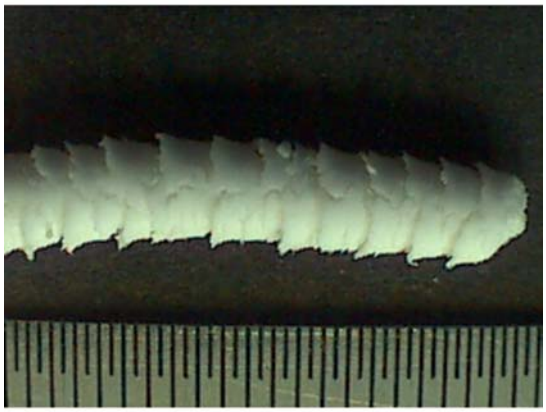

(b)

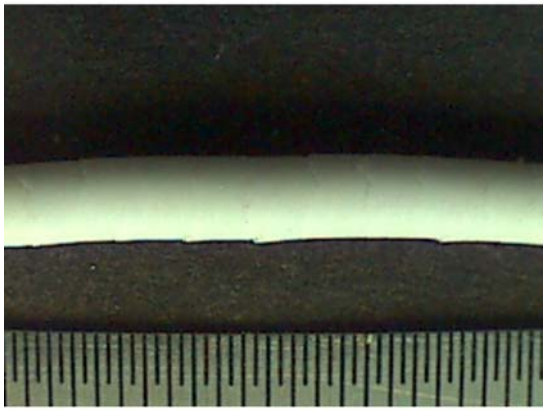

(c)

Figure 10 Extrudates of 50 wt% water-MCC extruded at a $V = 140$ mm s^{-1} through a 3 mm diameter die with L/D = [a] 1, [b] 2 and [c] 4.

$L/D = 8$ and 16, the modal diameter has increased, occurring within the size fraction 1.70–2.00 mm (2.2–2.6 mm wet). For the highest velocity, the distributions are similar for all die lengths, and show a bimodality with the modal diameters occurring within the size fractions of 0.71–1.00 mm and 1.40–1.70 mm.

For the 1 mm diameter dies, the extrudates fractured forming cup shapes for all L/D values studied, and all the extrudates had flares of $y = 1.25$ mm and fracture spacings of $x = 0.5$ mm, as shown in Fig. 18 ($\delta = 0.98$ mm from Eq. (1)). No knuckle-bones or smooth extrudates were formed. The fractures are visibly more severe for the shortest die, although once again this could not be monitored quantitatively to within measurement error. The morphology of the pellets was similar at each die length, being that of well-formed spheres (no visible dimples) and ellipses, with some dumb-bells and cylinders present (e.g. see Fig. 19). The corresponding pellet size distributions are displayed in Fig. 20, and are fairly similar for each die length, with the modal diameter occurring within the size fraction 1.00–1.18 mm (1.3–1.5 mm wet).

4. Discussion

Although there has been much debate regarding the origins of extrusion defects in polymer melts, literature discussing the cause of fractures in paste extrusion has, until fairly recently, been sparse. Russell *et al*. [36] showed that the extrusion pressure measured at the die for a range of stiff pastes undergoing regular fracture contained distinct peaks in the frequency spectrum, indicating a cycling of stresses during fracture, the period of which was similar to the occurrence of fracture reported by Domanti and Bridgwater [22]. Russell *et al*. observed that the frequency peak became more distinct as the apparent severity of the fracture and the magnitude of the die wall shear stresses increased. The apparent severity of fracture increased with extrusion velocity, i.e. larger tensile shear stresses. The use of a PTFE coated die land greatly reduced the severity of fracture, in some cases eliminating it altogether. These results suggested that the paste appeared to rupture only when the stresses exceeded a certain crack onset threshold for the material. The results presented here indicate that fracture onset and mode are not simple functions of parameters such as geometry and wall shear stress.

Pharmaceutical studies had also proposed that certain rheological material parameters may influence the surface impairment of paste extrudates, and hence the final shape and size distribution of the spheronised product. For example, Harrison *et al*. [37] suggested that these may be the upstream pressure loss and the mean die wall shear stress. Raines [38] characterised MCC/lactose pastes using the Benbow and Bridgwater [39] approach, and observed that formulations with low values of the initial bulk yield stress and initial paste-die wall shear stress were more likely to produce extrudates with surface defects. The following discussion attempts to describe the fracture mechanisms involved in the current MCC paste extrusion experiments, and what effect the processing and material parameters have on them as characterised by the change in fracture geometry. The discussion then addresses how the extent of fracture is related to the quality of the spheronised product in terms of the pellet morphology, size and size distribution.

4.1. Fracture mechanism

The area with the most published work on extrusion defects is polymer melt extrusion, in which shark-skinning is usually associated as originating at the die exit. One explanation for shark-skinning is that it is caused by the rupturing of material at the die exit due to high tensile stresses (e.g. [27, 28, 29]). Benbow *et al*. [40] were one of the first to suggest such a die exit

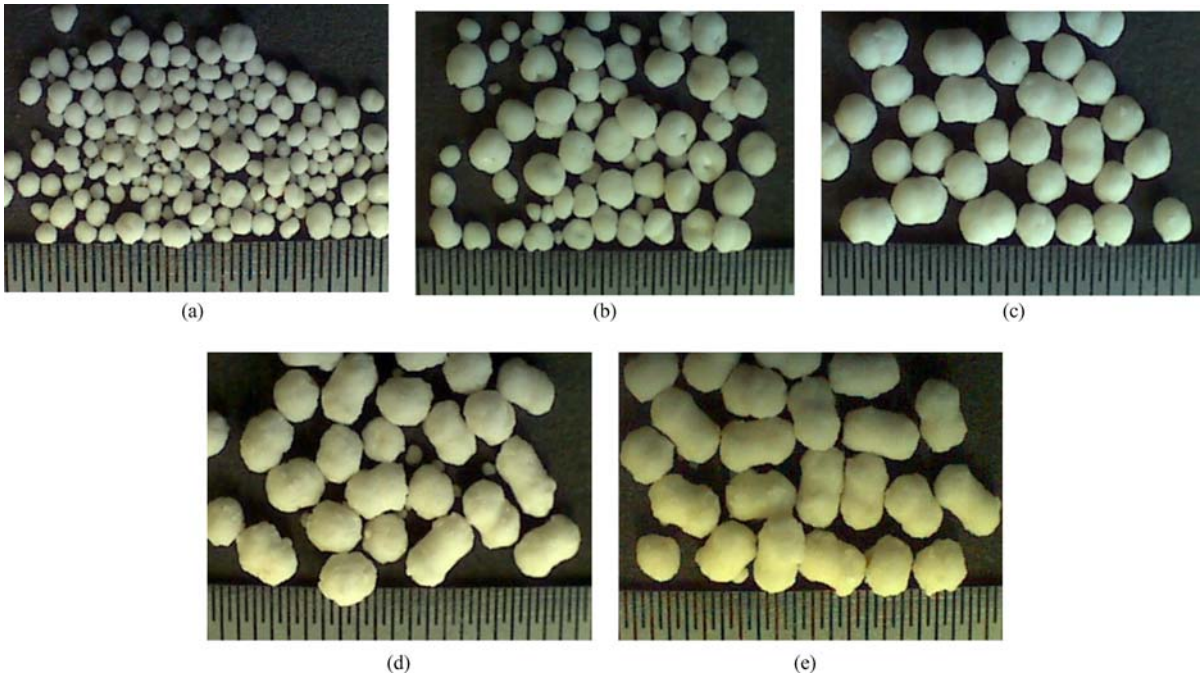

Figure 11 Dried pellets obtained from the spheronisation of 50 wt% water-MCC extruded at $V = 140$ mm s^{-1} through a 3 mm diameter die with L/D = [a] 1, [b] 2, [c] 4, [d] 8 and [e] 16.

mechanism. They argued that a polymer melt flowing at steady state through a die has a radial distribution of axial velocities initiated by frictional effects at the die wall, with the centreline material travelling at a maximum velocity. However, when the extrudate is free of the die, it travels at a constant average velocity, and so upon exiting the die, the central material decelerates whilst the surface material accelerates. Richardson [41] used mass conservation to show that this acceleration creates a tension in the surface layer, whilst the decelerating centreline material is compressed. If the tension in the surface layer thus exceeds a critical stress, the material fractures. Benbow *et al*. [40] also mention that further stresses will be induced by the radial elastic recovery of the extrudate on exiting the die. This tension/compression effect was also proposed by Nickell *et al*. [42] who used a finite element method to model polymer melt extrusion, and was confirmed experimentally by Osakada *et al*. [43] and Polyakov *et al*. [44] for metal extrudates. The existence of exit zone stress concentrations in polymer melts has been confirmed by birefringence experiments [45] and numerical modelling [46]. Domanti and Bridgwater [47] used a finite element method and a perfect elasto-plastic material model to describe ceramic paste extrusion, and they observed compressive and tensile stresses at the centre and surface of the extrudate respectively.

Similar surface stretching mechanisms were proposed by Yamada *et al*. [48] for the cause of fir-tree cracks in metal alloy extrusion, Cogswell [49] for polymer melts, and more recently by Kulikov and Hornung [50, 51] to explain extrusion defects of a clay powder/mineral oil mixture. Fiorentino *et al*. [25] suggested a slightly different mechanism for circumferential cracks occurring in beryllium metal extrudates. As the extrudate exits the die, it expands elastically. The stress discontinuity causes the surface fibres to bend which results in longitudinal tensile stresses. These coupled with residual axial tensile stresses developed at the die inlet deformation stage, and those due to friction, cause cracking.

The idea of tension/compression effects within a material exiting a die was embraced by Harrison [15] and Harrison *et al*. [32] as an explanation for fracture in pharmaceutical paste ram extrusion. They argued that higher extrusion velocities resulted in higher wall shear stresses, thus increasing the tension effects at the surface of the extrudate, leading to more severe fractures (as seen in the present work). In order to explain the effect of the die length, they used the concept of wall slip, in which shearing occurs in a uniform lubricating layer (liquid or liquid/solid) adjacent to the die wall, with the central core of the extrudate flowing as a plug. For paste entering a die land, there will be a finite entry length before this layer can fully develop. For short dies, the entry length will be longer than the die length, and hence the flow within the die will be unsteady. The thickness of the lubricating layer would therefore vary within the die, with zero thickness creating a stick condition, and some finite thickness allowing for maximum slip. For the extreme case of stick, the material adjacent to the die wall will be static, and the heightened velocity gradient of the flow profile would intensify the stretching of the surface layer, thus increasing the severity of fracture. Raines [38] calculated the lubricating layer thickness for the ram extrusion of water-based MCC/lactose pastes using a paste flow mechanics approach [52]. She related the film thickness to the extrudate quality at constant shear rate, with the thickest layer resulting in a smooth surface, and the thinner layers resulting in surface impairments. However, Tomer *et al*. [53] used magnetic resonance imaging to measure the water distribution within MCC paste extrudates ($L/D = 4$, $V = 54$ and 540 mm s^{-1}), and found that

the distribution was "surprisingly uniform" across the diameter, although it should be noted that the samples were examined *ex situ*.

There are four main questions that can be asked about the nature of the extrudate fractures seen in the present work: (a) why are the fractures circumferential and concavely shaped upwards in the direction of paste flow; (b) what determines the apparent severity of the fractures; (c) why do the fractures occur periodically; and (d) what determines the spacing of the fractures, as defined by x in Fig. 1? These questions are now addressed.

4.1.1. The shape

The concave circumferential shape of the fractures is similar to that reported by Train [54] in the ejection of pressed compacts of magnesium carbonate powder. These ejection cracks were explained in terms of the radial and axial strain relief of the compact whilst exiting

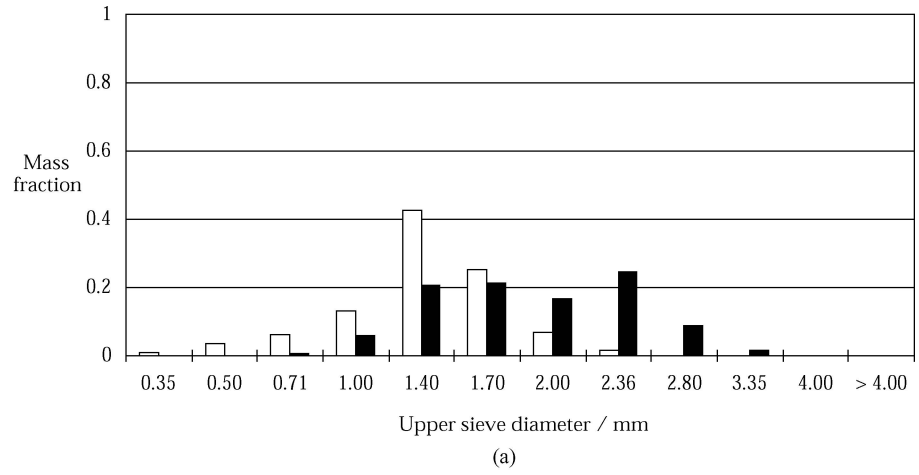

(a)

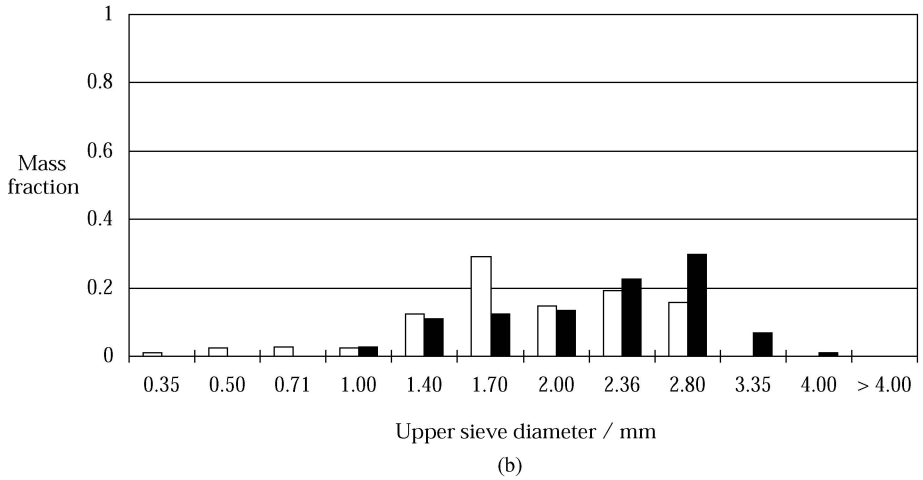

(b)

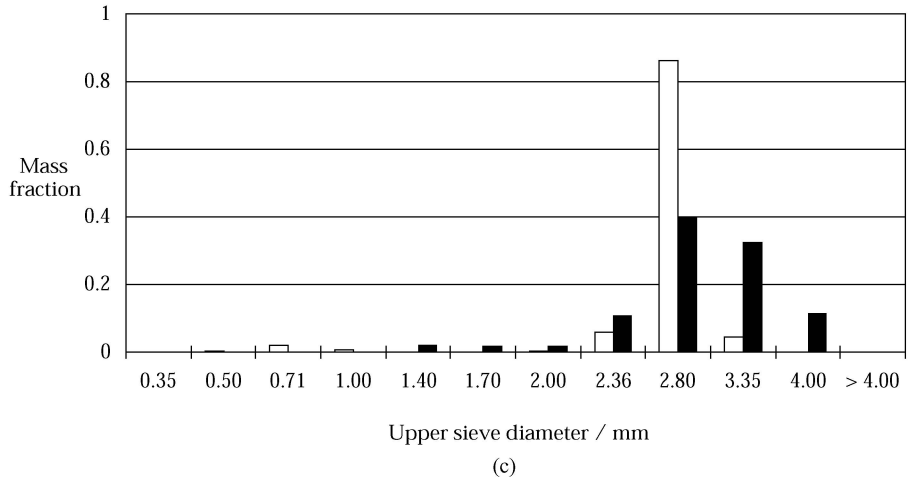

(c)

Figure 12 Size distributions in terms of mass fraction of dried pellets obtained from the spheronisation of 50 wt% (□) and 55 wt% (■) water-MCC extruded at $V = 140$ mm s^{-1} through a 3 mm diameter die with L/D = [a] 1, [b] 2, [c] 4, [d] 8 and [e] 16. (*Continued*.)

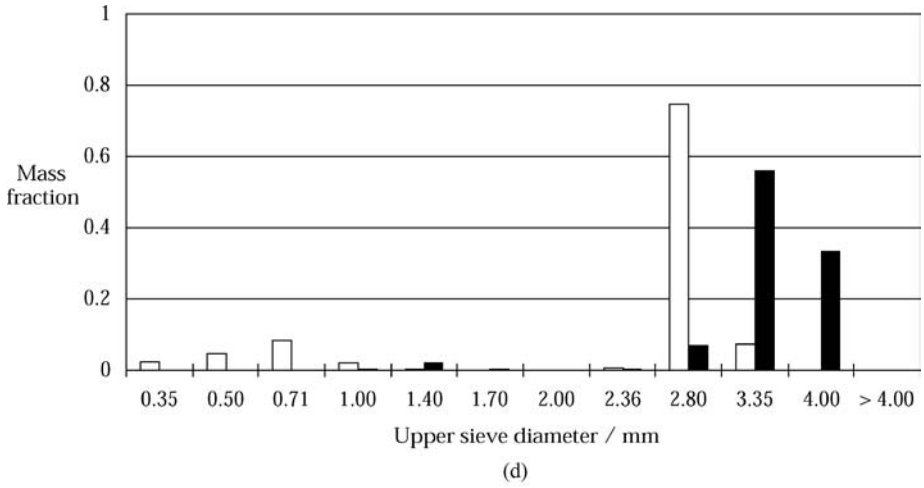

(d)

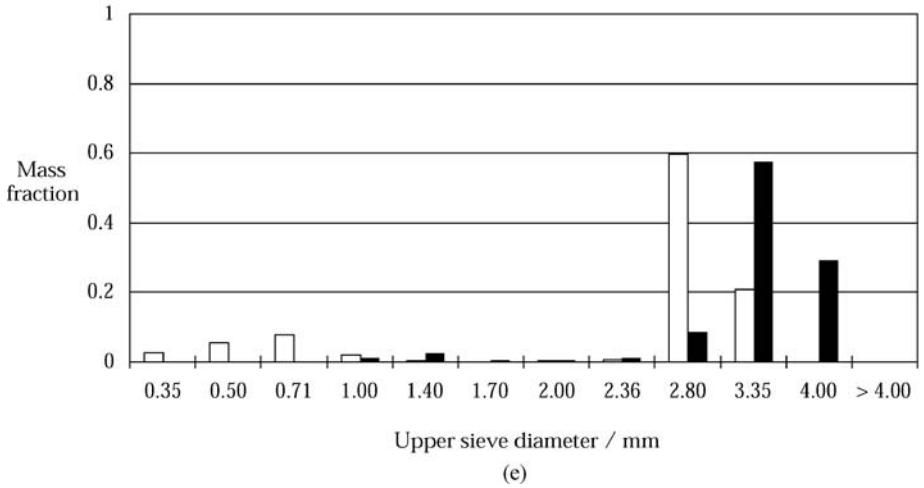

(e)

Figure 12 (*Continued*).

the die, the resultant of which created a rupture along a concave-shaped stress path. This was commented upon further by Long [55] for the ejection of metal powder compacts, and more recently by Nam *et al*. [56] for compacts of spray dried alumina agglomerates. Long argued that the formation of the stress concentrations were a result of the compact being restricted from expanding axially at the die wall due to friction, whereas the centreline of the compact was relatively free to move. A crack would temporarily relieve the stress concentration in the material immediately upstream, but as the compact continued to exit the die, the stresses would begin to build up again in a new uncracked region. In this way, a series of concave cracks would be formed. It is thought that similar stress concentrations may be established during paste extrusion, which therefore generate a series of concave shaped fractures. Domanti and Bridgwater [47] have also reported similar concave fractures for alumina/starch pastes in rectangular slot dies. By using transparent die material they were able to confirm that the cracks initiated at the die exit.

4.1.2. The severity

Work is done on the paste as it undergoes convergent flow at the die entrance and shear along the die land. Much of the former contribution will be plastic work, arising from re-alignment and modification of particles, but some will be stored in the form of elastic energy, to be released when the constraining factors (e.g. the die walls) are removed. Expansion of the paste can occur both radially and axially upon exiting the die, the former being constrained by the die walls, and the latter being constrained by both the wall friction (for paste adjacent to the die wall) and the internal friction of the paste material. The radial expansion can be visually quantified by comparing the extrudate flare, y, with the actual die diameter. For large values of y, the fracture appears to be more severe (as represented by α' in Table II). Table II shows that y increases with decreasing L/D and increasing extrusion velocity, both of which also tend to produce knuckle-bone fractures.

The particle matrix undergoes rearrangement during the die entry phase and this can result in several changes, the most relevant here being consolidation which reduces the number of crack initiation sites (e.g. by breakdown of agglomerates or reduction in void sizes). For a given extrusion velocity, larger extrusion pressures (i.e. L/D values) are likely to result in a paste which is less likely to fracture, i.e. it undergoes a hardening process. Russell *et al*. [36] suggested that the increase in die length will increase the compressive stress in the deforming zone, which may result in a less brittle material which would reduce fractures when extruded.

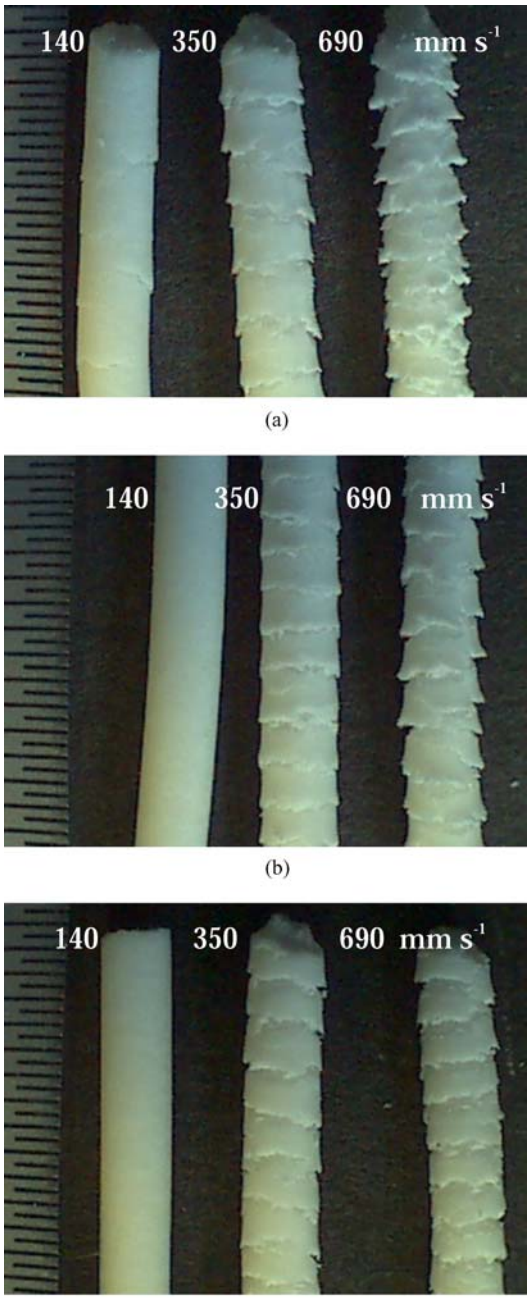

Figure 13 Extrudates of 50 wt% water-MCC extruded at $V = 140$, 350 and 690 mm s^{-1} through a 3 mm diameter die with $L/D =$ [a] 4, [b] 8 and [c] 16.

Thus for short dies the material contains a higher density of crack initiation sites, and hence the radial and axial strain released is more significant. This postulation is supported by the reduction in fracture severity observed as L/D increases. Longer die lands also give the paste more time to develop lubricating layers at the wall and relax extensional strains resulting from the die entry (e.g. by further particle re-alignment), *viz.* an entry length effect. It is not possible to separate these two components reliably within the experiments performed here. It is noteworthy, however, that plots of average extrusion pressure *vs.* L/D (i.e. Bagley plots) for almost all series of tests were linear, indicating that the wall shear stress was uniform, and that fracture is a strong micro-mechanical response to stress-strain conditions imposed upon the material.

Increasing the die land velocity increases the wall shear stress in the die land (evident from the Bagley plots). If the die entry contribution is strain-rate independent (e.g. there is no redistribution of liquid, which is a reasonable point borne out by the extrusion pressure data), then the fracture behaviour at different velocities is the response of similarly 'hardened' material to different shear stress/strain and elastic energy conditions. Increasing the velocity uniformly resulted in greater severity of fracture, which is consistent with both die land entrance effect, and wall shear stress/elastic energy explanations.

4.1.3. The periodicity

One explanation for the periodicity shown by the fractures is that a type of stick-slip mechanism is occurring within the die land prior to exit. This mechanism could occur either upstream at the die entry, or at the die exit, and would be initiated by friction at the die-paste interface. However, Domanti and Bridgwater [22] reported a periodic fracture spacing of $D/2$ for alumina-glucose paste extrusion with L/D varying between 1/6 and 16. The fact that fracture still occurred at a relatively small aspect ratio of 1/6 implies that die wall friction is not the major cause of the periodicity. For metal alloy extrusion, Yamada *et al.* [48] suggested that any stick-slip mechanism was itself caused by the stress relief produced during cracking. For the present MCC paste extrusion, it is suggested that the fracture periodicity is established purely by the geometrical layout of the cracks, which is itself determined by the shape of the stress rupture path upstream in the paste.

4.1.4. The spacing

Domanti and Bridgwater [22] reported that the spacing of periodic circumferential extrudate fractures is approximately equal to $D/2$ for many paste systems and geometries. This spacing was also observed with the present MCC paste extrusion for dies of diameter 1 and 2 mm, and can be explained by assuming a hydrostatic release of the stresses within the paste upon exit from the die. (Work performed by Amarasinghe and Wilson [23] indicated that ceramic pastes transmit stresses in a hydrostatic manner.) This creates a rupture path at an angle of $\theta = 45^\circ$ for a material with isotropic tensile yield properties. As the crack propagates, it relieves the stresses in the paste adjacent to it bounded by the die wall, and the fractured segment is allowed to expand both axially and radially upon leaving the die exit. The next fracture will thus be initiated in an uncracked portion of paste bounded by the die wall upon reaching the die exit; this portion of paste occurs at a distance of $D/2$ from the first crack initiation point. However, for the 3 mm diameter die, the fracture spacing is not simply defined by $D/2$, but varies from $D/3$ to $3D/4$ (see Table II). This range of values can be explained by the development of non-equal radial and axial strains, which occur if either a hydrostatic stress is released in a paste with non-isotropic tensile yield properties, or the radial and axial stresses are themselves non-equal.

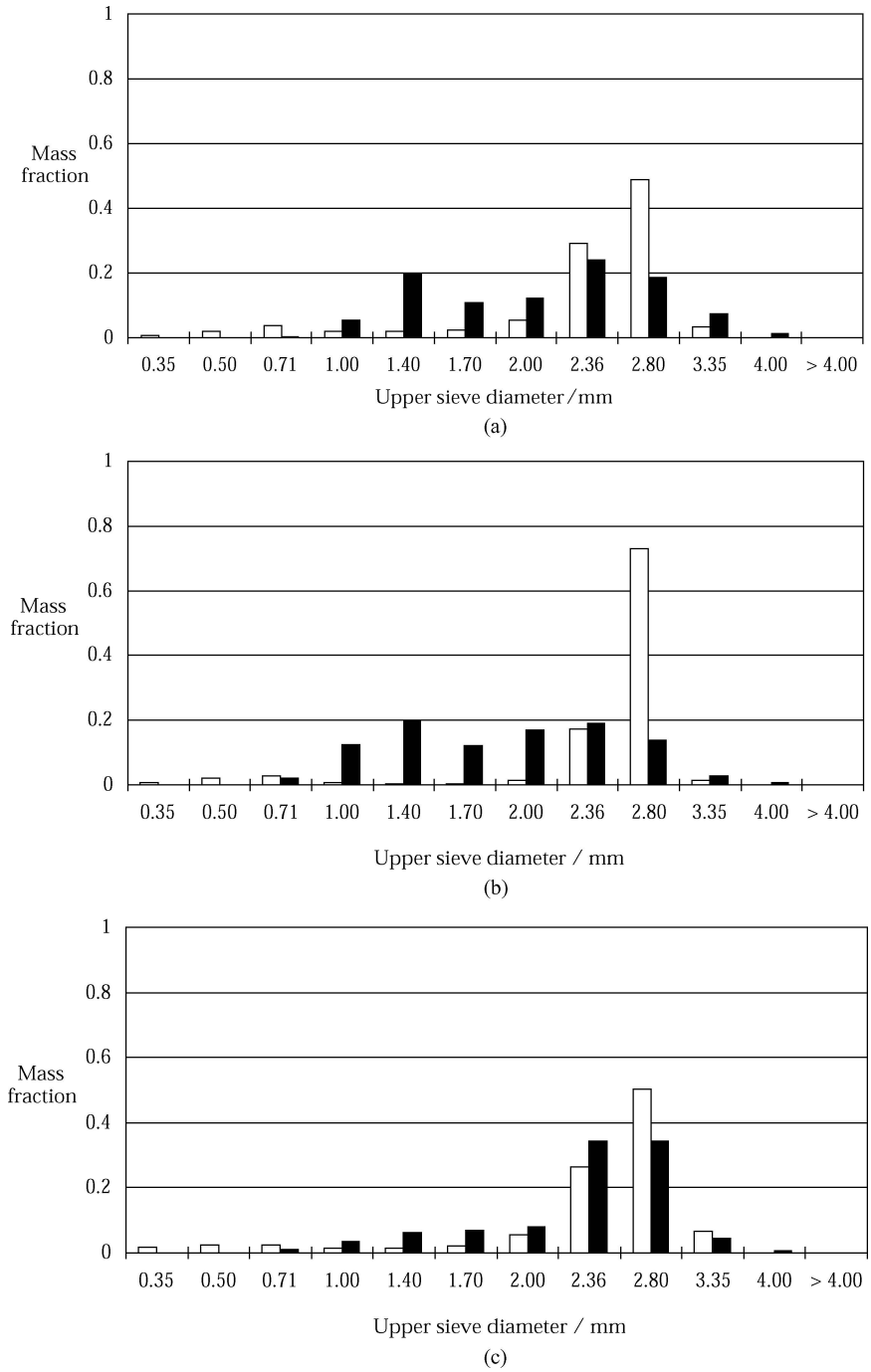

Figure 14 Size distributions in terms of mass fraction of dried pellets obtained from the spheronisation of 50 wt% (□) and 55 wt% (■) water-MCC extruded at $V = 690$ mm s^{-1} through a 3 mm diameter die with $L/D =$ [a] 4, [b] 8 and [c] 16.

Part (b) of this discussion explained how the magnitude of the radial and axial strains released at the die exit may be affected by the extrusion velocity and the die length. A summary of the proposed fracture mechanism is now outlined in Fig. 21. Two extreme fracture geometries are shown, which in turn produce [a] knuckle-bone and [b] cup shaped fractures. If the fracture angle $\theta > 45^\circ$, then the radial strain (ε_r) is greater than that of the axial (ε_z) and knuckle-bones are produced. As a consequence the fracture spacing $x < D/2$. This fracture geometry occurs, in general, for small L/D values or high extrusion velocities (see Table II) as discussed in parts (b) and (d) above. As L/D increases, or the extrusion velocity decreases, if the rate of decrease in radial strain is more than that of the axial, then a point will be reached when the radial strain release will be less than that of the axial. This produces a fracture angle $\theta < 45^\circ$ and a subsequent fracture spacing of $x > D/2$, which corresponds to cup shaped fractures. Since a finite amount of energy is released and hence expended during crack growth, the crack is unable to fully propagate across the central core of the paste extrudate. This, coupled with a further decrease in θ and an increase in spacing x will result in extrudates with faint surface fractures, until eventually for either very long dies, or low extrusion velocities, smooth extrudates will be formed, since both the radial and axial strain release will be minimal.

Harrison *et al.* [32] reported that surface impairments were more pronounced for MCC/lactose paste with a

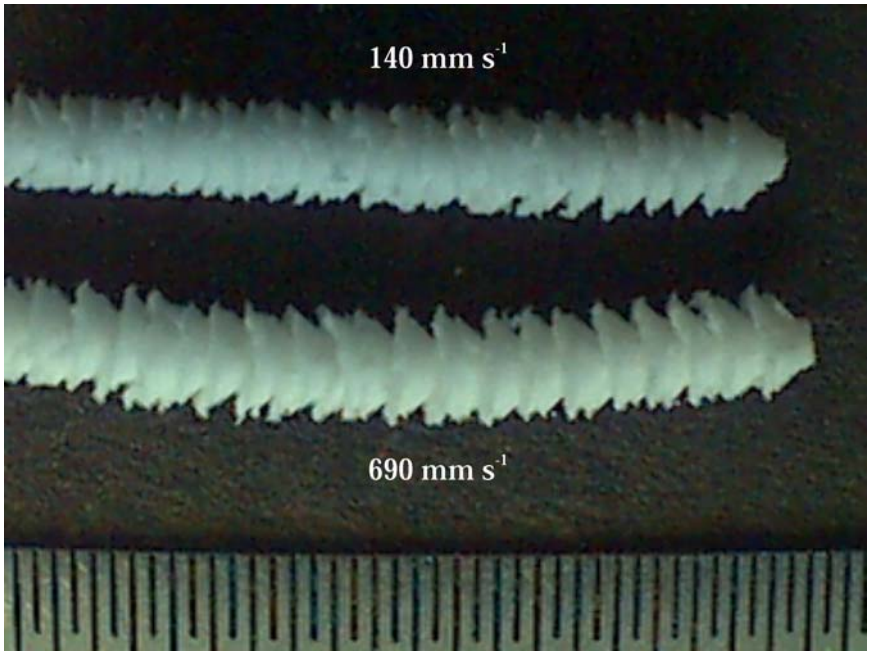

Figure 15 Extrudates of 55 wt.% water-MCC extruded at $V = 140$ and 690 mm s^{-1} through a 2 mm diameter die with $L/D = 8$.

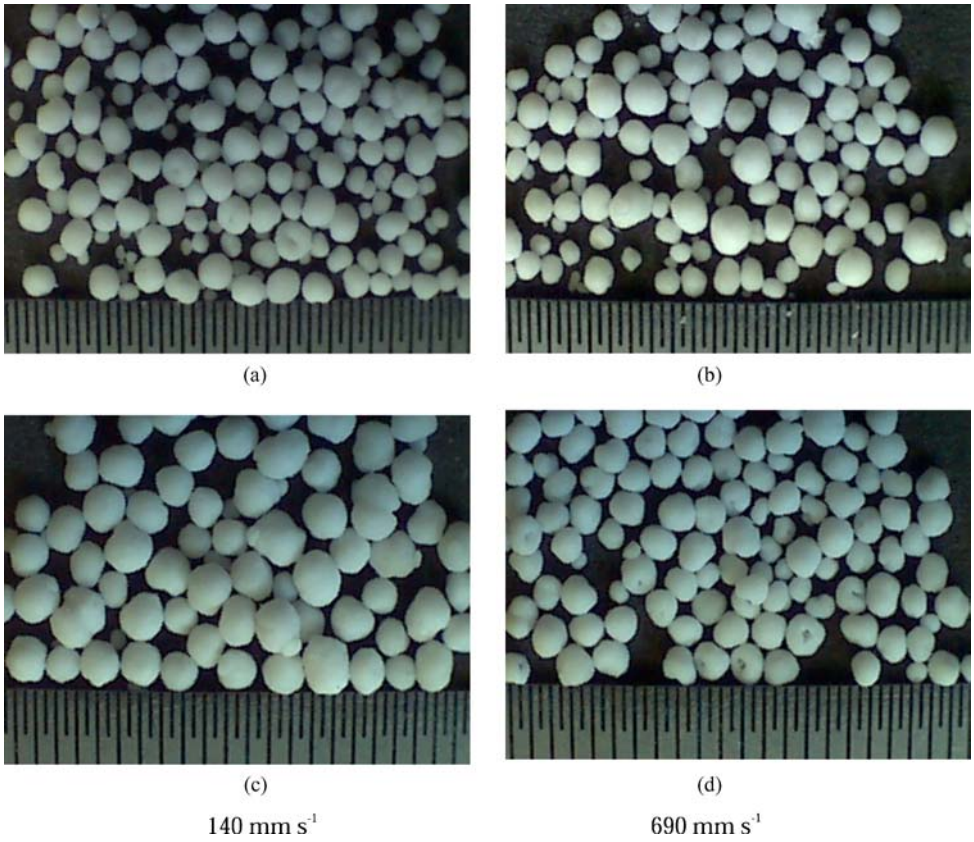

Figure 16 Dried pellets obtained from the spheronisation of 55 wt.% water-MCC extruded at $V = 140$ mm s^{-1} (left hand column) and 690 mm s^{-1} (right hand column) through a 2 mm diameter die with L/D = [a&b] 1 and [c&d] 16.

higher water content, which they attributed to a reduction of forces required to maintain a smooth surface. Table II shows that the radial expansion of the 55 wt% water-MCC paste is greater than that of the 50 wt% paste for the three longer dies, although the opposite effect occurs for the two shortest dies. This suggests a larger variation in elastic response for the drier paste under the extrusion conditions studied. The 50 wt% paste also has a tendency to produce cup fractures rather than knuckle-bones when compared with the corresponding 55 wt% extrusion. This implies that the radial strain release is less than that of the axial, which is probably due to the increased compressive stress in the deformation zone and the increase in wall shear stress (as listed in Table I). The smooth extrudates are less than 3 mm in diameter, which implies the formation of a

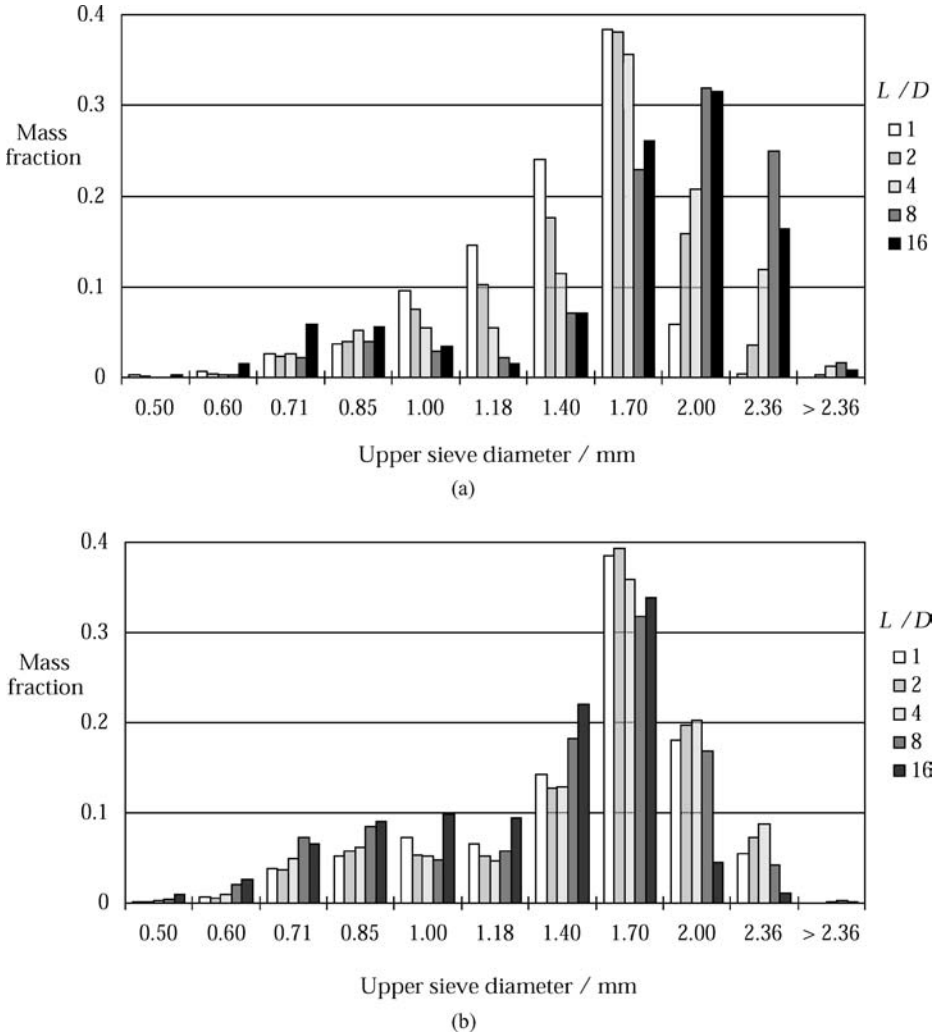

Figure 17 Size distributions in terms of mass fraction of dried pellets obtained from the spheronisation of 55 wt.% water-MCC extruded through a 2 mm diameter die with L/D = 1, 2, 4, 8 and 16 at V = [a] 140 and [b] 690 mm s^{-1}.

fully developed liquid slip layer. The preferential ability of the drier paste to generate this layer may be a result of it experiencing higher stresses within the die land, which would increase the pore pressure and hence enhance the movement of the liquid phase towards the die wall.

No definitive trend can be seen for the fracture shape with respect to die diameter. The comparison is complicated by the inability to accurately assess the shear rate of the paste at the die wall, and also by the inability to monitor whether a slip layer is being formed. Also the accuracy of measuring the geometric features such as the fracture spacing and extrudate flare for the smaller diameter dies is compromised by the irregularity of the fracture shapes themselves, as discussed by Domanti and Bridgwater [22]. This could be ameliorated by the use of other measuring systems, such as laser profilometry. Hence at present the authors cannot offer any satisfactory explanation as to why the 2 mm diameter dies only produced knuckle-bone fractures, whereas the corresponding 3 mm diameter extrusions at equal L/D and die land velocities produced cup fractures and smooth extrudates. For the highest die land velocity and $L/D = 2, 4$ and 8, the radial expansion of the fractured extrudates is 42, 50 and 25% for the 3, 2 and 1 mm diameter dies respectively, with the lowest amount of radial expansion corresponding to cup fractures. The reason why the radial expansion is smaller for the 1 mm dies, whereas one could expect more due to the increase in extrusion ratio and hence the resulting radial extension, is not fully understood and an area for further work.

4.2. Fracture geometry and spheronisation mechanism

During spheronisation, the extrudate initially breaks into its individual fracture segments, if any, which are then further shaped by the rotating friction plate. The experimental results show that the type of fracture shape affects the spheronised pellet morphology, size and size distribution. For example, the 55 wt% paste extruded through a 3 mm diameter die with $L/D = 4$, 8 and 16 produces a change in the fracture shape as the velocity increases from 140 mm s^{-1} (cup, smooth, smooth) to 350 mm s^{-1} (knuckle-bone, cup, cup). The transition in fracture shape clearly affects the pellet size distribution, as illustrated in Fig. 8c–e.

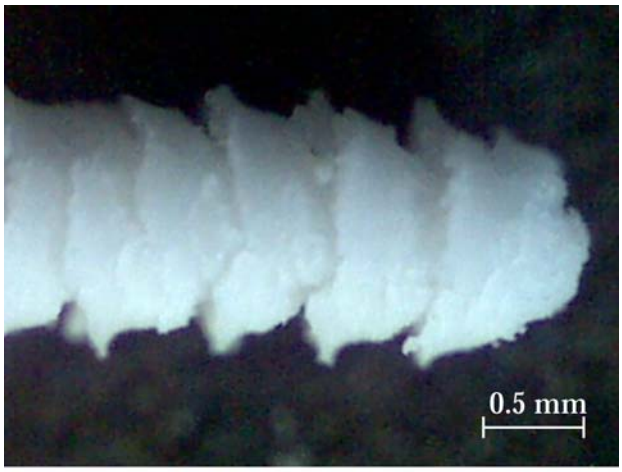

(a)

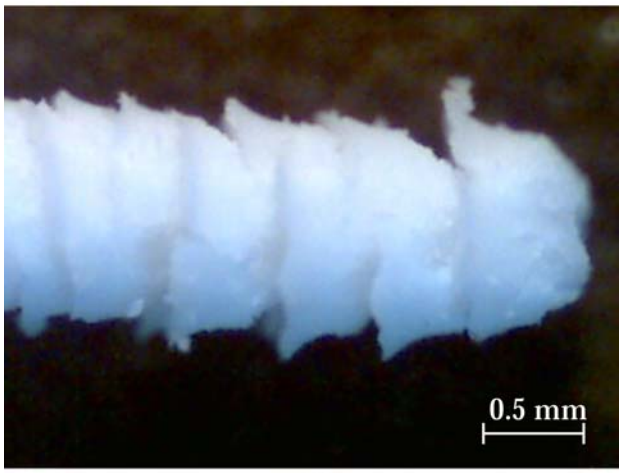

(b)

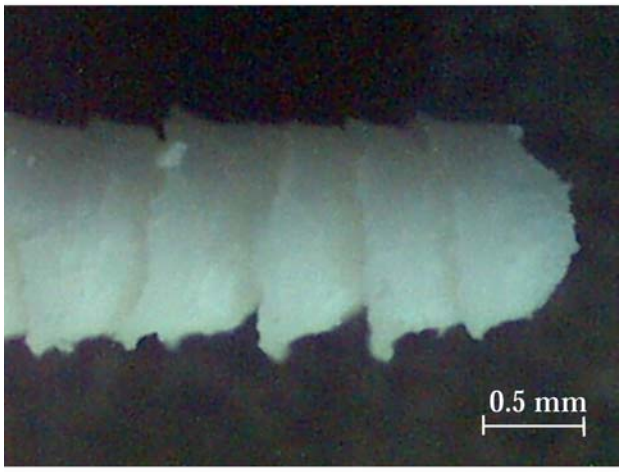

(c)

Figure 18 Extrudates of 55 wt.% water-MCC extruded at $V = 690$ mm s^{-1} through a 1 mm diameter die with L/D = [a] 2, [b] 4 and [c] 8.

For the knuckle-bone fractures, the pellets generated are spherical and have a wide, sometimes bimodal, size distribution. The wide size range can be explained by fines that are created from the breakage of the ragged edges of the fracture segments, as shown in Fig. 2(a). The increase in the occurrence of dimpled spheres can be correlated with either a decrease in water content of the paste, or an increase in extrusion velocity, both

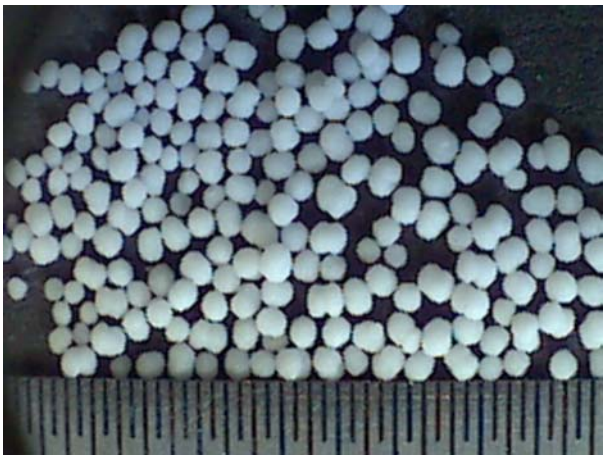

Figure 19 Dried pellets obtained from the spheronisation of 55 wt.% water-MCC extruded at $V = 690$ mm s^{-1} through a 1 mm diameter die with $L/D = 2$.

of which cause an increase in the value of the maximum extrusion diameter, y, for the two shortest dies (Table II). A dimpled sphere is formed by the skirts of the fracture segment folding over together [10], an example of which is displayed in Fig. 22. The drier paste generates more dimpled spheres since it is less plastic, and hence the wider skirts of the knuckle-bones cannot fold over fully and deform to eliminate the depression. As the extrusion velocity increases, the number of dimpled spheres increases since the knuckle-bone fractures produced have a larger skirt diameter due to the increase in radial expansion of the extrudate at the die exit, which also have difficulty in folding over completely.

Cup fractures produce visibly larger spherical pellets with a mono-modal, narrower size distribution (e.g. see Figs. 3c and 4). The morphology of the pellets and the narrowing of the size distribution implies that the cup type of fractured extrudate breaks down and deforms more regularly within the spheroniser. Less fines are produced since the fracture segment edges are less ragged.

Smooth extrudates, or those with faint surface fractures, are more resistant to breakage during spheronisation, and will initially fracture into short rods which are rounded off and compacted at the ends by the action of the rotating plate, thus forming dumb-bells. The number of dumb-bells increases with increasing L/D, decreasing extrusion velocity, or decreasing paste water content. Pellets are generated with typically mono-modal and narrow size distributions (e.g. see Fig. 4), which is not surprising since the sieving process only measures the minimum width of a pellet [57, 58], which in this case is equal to or greater than the initial extrudate diameter. For the 50 wt% paste, cylinders as well as dumb-bells were sometimes produced (e.g. see Fig. 11d and e), which suggests that the drier paste is less plastic since the ends of the pellets are unable to be rounded off to form dumb-bells.

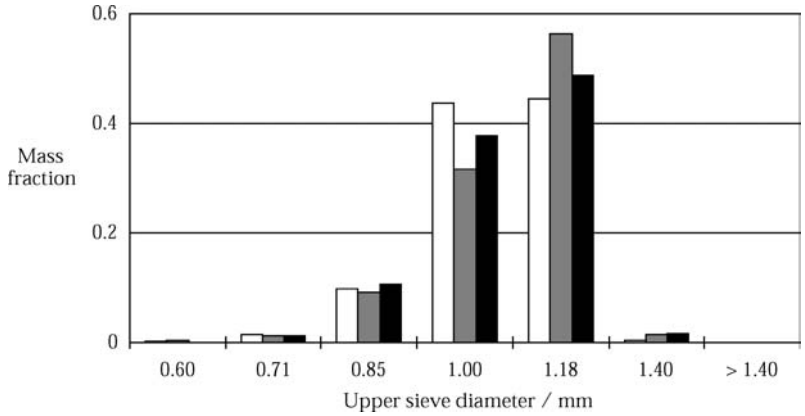

Figure 20 Size distributions in terms of mass fraction of dried pellets obtained from the spheronisation of 55 wt.% water-MCC extruded at $V = 690$ mm s^{-1} through a 1 mm diameter die with $L/D = 2$ (□), 4 (▒) and 8 (■).

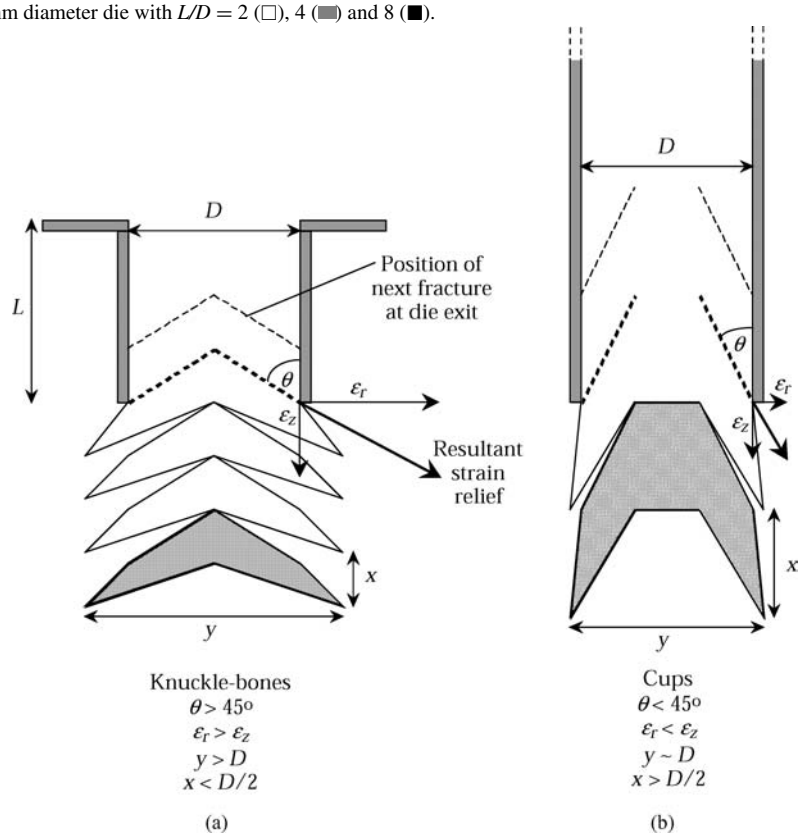

Figure 21 Schematic representation of the fracture mechanism occurring in [a] short dies (*e.g.* $L/D = 1$) and [b] intermediate length to long dies (e.g. $L/D = 4$ to 16).

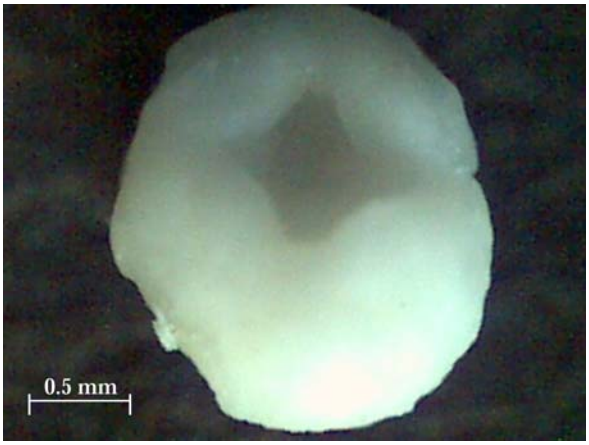

Figure 22 A dimpled dried pellet obtained from the spheronisation of 50 wt.% water-MCC extruded at $V = 690$ mm s^{-1} through a 3 mm diameter die with $L/D = 1$.

5. Conclusions

The relationships between extrusion behaviour and spheronisation performance of a typical pharmaceutical excipient formulation (MCC-water) have been investigated and related to the existing understanding of surface defect formation in pastes (wet powder masses) undergoing extrusion. The type of MCC paste extrudate circumferential fracture has been shown to affect the morphology, size and size distribution of the spheronised product.

Knuckle-bone fractures tended to produce pellet samples containing more fines due to the breakage of ragged edges, and spheres with more dimpled surfaces since the segments have difficulty in folding over completely in the spheroniser. Smooth extrudates tended to produce dumb-bells and cylinders since they cannot break up evenly in the spheroniser: extended operation

resulted in a wide range in sizes of spherical products. It appears that cup shaped fractures are desirable in order to produce well-formed spheres with a narrow size distribution, intimately related to the diameter of the die land *via* the spacing of fractures.

Fractures featured regular periodicity which, whilst constant for a given set of process conditions, increased with increasing L/D and decreasing extrusion velocity. The apparent severity of the fracture was related to the extent of the radial expansion of the extrudate, and decreased with increasing L/D and decreasing extrusion velocity.

We propose that the fracture geometry can be explained in terms of a mechanism based upon the extent of the release of axial and radial strains on the extrudate surface upon exiting the die. Fracture is postulated to be a micro-mechanical phenomenon related to the presence of crack initiators (duly suppressed by high consolidating stresses) and the tensile strains generated in the die land, which resonates with the conclusions of Domanti and Bridgwater [47] for ceramic paste extrusion. Thus for long dies and low extrusion velocities, the strains released will be minimal and a smooth extrudate will be formed. Knuckle-bone fractures are formed with short dies at all extrusion velocities, and with intermediate length dies at higher velocities, and are thought to be a result of the radial strain release being greater than that of the axial. Cup fractures are formed with intermediate length dies at low velocities, and with the longest dies at high velocities, and are thought to be a result of the axial strain release being greater than that of the radial. This suggests that the change in die length (and hence the paste crack initiator density) has more influence upon the extent of the radial strain than that of the axial, whereas the change in extrusion velocity (and hence the die wall shear stress) has more influence upon the extent of the axial strain than that of the radial.

Nomenclature

d	diameter of extrudate section (see Fig. 1)	[m]
D	die diameter	[m]
L	die length	[m]
V	mean velocity of paste in die land	[ms^{-1}]
x	fracture spacing (see Fig. 1)	[m]
y	extrudate flare (see Fig. 1)	[m]
α	extrudate skirt angle (see Fig. 1)	
α'	a representation of the severity of fracture, given by $\tan^{-1}\left(\frac{y-3}{2x}\right)$	
δ	diameter of sphere	[m]
ε_r	radial strain	
ε_z	axial strain	
θ	extrudate fracture angle (see Fig. 1)	

6. Acknowledgments

The authors would like to thank Professor Mike Newton for helpful discussions and Professor John Bridgwater for encouragement and support. Digital image analysis of the MCC pellets was kindly performed by Christison Particle Technologies, Gateshead, UK.

References

1. L. HELLÉN and J. YLIRUUSI, *Int. J. Pharm.* **96** (1993) 217.
2. A. D. REYNOLDS, *Manuf. Chem.* **41** (1970) 40.
3. M. J. GALMEN *Manuf. Chem.* **6** (1985) 55.
4. K. E. FIELDEN, J. M. NEWTON and R. C. ROWE, *Int. J. Pharm.* **81** (1992) 205.
5. J. W. CONINE and H. R. HADLEY, *Drug Cosm. Ind.* **106** (1970) 38.
6. R. C. ROWE, *Pharm. Int.* **6** (1985) 119.
7. S. R. CHAPMAN, R. C. ROWE and J. M. NEWTON, *J. Pharm. Pharmacol.* **40** (1988) 503.
8. P. KLEINEBUDDE, M. SCHRÖDER, P. SCHULTZ, B. W. MÜLLER, T. WAALER and L. NYMO, *Pharm. Dev. Technol.* **4**(3) (1999) 397.
9. S. GALLAND, B. BATAILLE, M. DELALONDE, T. RUIZ, N. BENNACER and C. DUPUY, *Trans. I.Chem.E.* **81**(A) (2003) 1237.
10. L. BAERT and J. P. REMON, *Int. J. Pharm.* **95** (1993) 135.
11. D. BAINS, S. L. BOUTELL and J. M. NEWTON, *ibid.* **69** (1991) 233.
12. J. F. PINTO, G. BUCKTON and J. M. NEWTON, *Int. J. Pharm.* **83** (1992) 187.
13. *Idem. ibid.* **97** (1993) 79.
14. G. TOMER and J. M. NEWTON, *Int. J. Pharm.* **182** (1999) 71.
15. P. J. HARRISON, Extrusion of wet powder masses Ph.D. Thesis (University of London, 1982).
16. J. M. NEWTON, *STP. Pharma.* **6** (1990) 396.
17. L. HELLÉN, L. RITALAX, J. YLIRUUSI, J. PALMROOSX and E. KRISTOFFERSSON, *Pharm. Techn. Int. Biophys.* **4** (1992) 50.
18. L. BAERT, J. P. REMON, J. A. C. ELBERS and E. M. G. VAN BOMMEL, *ibid.*. **99** (1993) 7.
19. C. VERVAET, L. BAERT, P. A. RISHA and J. P. REMON, *Int. J. Pharm.* **107** (1994) 29.
20. A. M. JUPPO, L. HELLÉN, V. PULLINEN-STRANDER, K. KALSTA, J. YLIRUUSI and E. KRISTOFFERSSON, *Eur. J. Pharm. & Biopharm.* **44** (1997) 205.
21. A. T. J. DOMANTI, Surface Fracture in Paste Extrusion Ph.D. Thesis (University of Cambridge, 1998).
22. A. T. J. DOMANTI and J. BRIDGWATER, *Trans. I.Chem.E.* **78**(A) (2000) 68.
23. A. D. U. S. AMARASINGHE and D. I. WILSON, *Trans. IChemE.* **76**(A) (1998) 3.
24. B. D. RUSSELL, J. LASENBY, S. BLACKBURN and D. I. WILSON, *Powder Tech.* **132** (2003) 233.
25. R. J. FIORENTINO, B. D. RICHARDSON and A. M. SABROFF *Metal Forming* **36** (1969) 243.
26. D. S. KALIKA and M. M. DENN, *J. Rheol.* **31**(8) (1987) 815.
27. N. EL KISSI and J.-M. PIAU, *J. Rheol.* **38**(5) (1994) 1447.
28. S.-Q. WANG, P. A. DRDA and Y.-W. INN, *J. Rheol.* **40**(5) (1996) 875.
29. C. VENET and B. VERGNES, *ibid.* **41**(4) (1997) 873.
30. L. HELLÉN, J. YLIRUUSI, E. MUTTONEN and E. KRISTOFFERSSON *Pharm. Techn. Int.* **5** (1993[a]) 44.
31. L. HELLÉN, J. YLIRUUSI, P. MERKKU and E. KRISTOFFERSSON, *Pharm. Techn. Int.* **5** (1993[b]) 38.
32. P. J. HARRISON, J. M. NEWTON and R. C. ROWE, *J. Pharm. Pharmacol.* **37** (1985[a]) 81.
33. M. S. MESIHA and J. VALLÉS, *Drug Dev. Ind. Pharm.* **19**(8) (1993) 943.
34. A. S. BURBIDGE, J. BRIDGWATER and Z. SARACEVIC, *Trans. I. Chem.E.* **73**(A) (1995) 810.
35. S. L. ROUGH, J. BRIDGWATER and D. I. WILSON, *Intl. J. Pharm.* **204** (2000) 117.
36. B. D. RUSSELL, S. BLACKBURN and D. I. WILSON, *J. Mat. Sci.* (2004).
37. *Idem., ibid.* **37** (1985[b]) 686.

38. C. L. RAINES, The extrusion of various formulations of microcrystalline celluloses Ph.D. Thesis (University of London, 1990).
39. J. J. BENBOW and J. BRIDGWATER, "Paste Flow and Extrusion. (Clarendon Press, Oxford, UK, 1993).
40. J. J. BENBOW, R. H. BROWN and E. R. HOWELLS, "Coll. Int. Rheologie" (Paris, 1960) 65.
41. S. RICHARDSON, *Rheol. Acta* **9** (1970) 193.
42. R. E. NICKELL, R. I. TANNER and B. CASWELL, *J. Fluid Mech.* **65** (1974) 189.
43. K. OSAKADA, N. SHIRASHI and M. OYANE, *J. Inst. Metals* **99** (1971) 341.
44. E. V. POLYAKOV, V. V. DAVYDOV and Y. S. KONJAEV, *J. Mechanical Working Technology* **16**(1) (1988) 31.
45. G. SORNBERGER, J. C. QUANTIN, R. FAJOLLE, B. VERGNES and J. F. AGASSANT, *J. Non-Newtonian Fluid Mech.* **23** (1987) 123.
46. B. TREMBLAY, *J. Rheol.* **35** (1991) 985.
47. A. T. J. DOMANTI and J. BRIDGWATER, *Ind. Eng. Chem. Res.* **43** (2004) 3750.
48. T. YAMADA, T. ABE, M. NOGUCHI and M. OYANE, *Bull. J.S.M.E.* **15**(84) (1972) 672.
49. F. N. COGSWELL, *J. Non-Newtonian Fluid Mech.* **2** (1977) 37.
50. O. L. KULIKOV and K. HORNUNG, *J. Non-Newtonian Fluid Mech.* **98** (2001) 107.
51. O. L. KULIKOV and K. HORNUNG, *J. Non-Newtonian Fluid Mech.* **107** (2002) 133.
52. J. J. BENBOW, E. W. OXLEY and J. BRIDGWATER, *Chem. Eng. Sci.* **42**(9) (1987) 2151.
53. G. TOMER, M. D. MANTLE, L. F. GLADDEN and J. M. NEWTON, *Int. J. Pharm.* **189** (1999) 19.
54. D. TRAIN, *J. Pharm. Pharmac.* **8** (1956) 745.
55. W. M. LONG, Radial pressures in powder compaction *Powder Metall.* **6** (1960) 73.
56. J. NAM, L. WENXIA and J. J. LANNUTTI, *Powder Tech.* **133** (2003) 23.
57. C. LUSTIG-GUSTAFSSON, H. K. JOHAL, F. PODCZECK and J. M. NEWTON, *Eur. J. Pharm. Sci.* **8** (1999) 147.
58. G. TOMER, F. PODCZECK and J. M. NEWTON, *ibid.* **231** (2002) 107.

Received 9 August 2004
and accepted 4 April 2005